MARTIN MARIETTA ENERGY SYSTEMS LIBRARIES
3 4456 0360445 5

ORNL-436
PHYSICS GENERAL

AEC RESEARCH AND DEVELOPMENT REPORT

DECLASSIFIED
CLASSIFICATION CHANGED TO:
BY AUTHORITY OF
BY

LABORATORY RECORDS
1954

ORNL SUMMER SHIELDING SESSION

Gale Young, Leader

A CRITICAL REVIEW OF ORNL SHIELD MEASUREMENTS: NEUTRON ATTENUATION

H. P. SLEEPER, JR.

OAK RIDGE NATIONAL LABORATORY
CENTRAL RESEARCH LIBRARY
DOCUMENT COLLECTION
LIBRARY LOAN COPY
DO NOT TRANSFER TO ANOTHER PERSON
If you wish someone else to see this document, send in name with document and the library will arrange a loan.
UCN-7969
(3 3-67)

OAK RIDGE NATIONAL LABORATORY
OPERATED BY
CARBIDE AND CARBON CHEMICALS CORPORATION
FOR THE
ATOMIC ENERGY COMMISSION

OAK RIDGE, TENNESSEE

[redacted]

ORNL - 436

This document consists of 4
pages. Copy 7 of 126,
Series a

Contract No. W-7405, eng 26 *

ORNL SUMMER SHIELDING SESSION

Gale Young, Leader

A CRITICAL REVIEW OF ORNL SHIELD MEASUREMENTS: NEUTRON ATTENUATION

H. P. SLEEPER, JR.

Date Issued: DEC 21 19

OAK RIDGE NATIONAL LABORATORY
OPERATED BY
Carbide and Carbon Chemicals Corporation
for the
Atomic Energy Commission
Post Office Box P
Oak Ridge, Tennessee

This [redacted]

[redacted]

*Explanation on page 3.

MARTIN MARIETTA ENERGY SYSTEMS LIBRARIES
3 4456 0360445 5

[redacted]

ORNL 436
Physics General

OAK RIDGE NATIONAL LABORATORY INTERNAL DISTRIBUTION:

1. G. T. Felbe[illegible] (C&CCC)
2. 706-A Library
3. 706-A Library
4. 706-B Library
5. Biology Library
6. Health Physics Library
7. Training School Library
8. Training School Library
9. Central Files
10. Central Files
11. Central Files
12. Central Files
13. J. A. Swartout
14. J. H. Gillette
15. A. Hollaender
16. J. H. Frye, Jr.
17. E. J. Murphy
18. C. N. Rucker
19. W. D. Lavers
20. A. M. Weinberg
21. J. A. Lane
22. R. N. Lyon
23. M. M. Mann
24. C. E. Larson
25. W. [illegible] Hume
26. E. [illegible]. Blizard
27. [illegible] K. Ergen
28. [illegible]entral Files (Off-Plant)
29. Central Files (Off-Plant)
30. Central Files (Off-Plant)
31. Central Files (Off-Plant)
32. Central Files (Off-Plant)
33. Central Files (Off-Plant)
34. Central Files (Off-Plant)
35. Central Files (Off-Plant)
36. Central Files (Off-Plant)

OAK RIDGE NATIONAL LABORATORY EXTERNAL DISTRIBUTION:

37-48. Argonne National Laboratory
49. Armed Forces Special Weapons Project
50-51. Atomic Energy Commission, Washington
52. Battelle Memorial Institute
53-56. Brookhaven National Laboratory
57-58. Bureau of Ships
59-62 Carbide and Carbon Chemicals Co[illegible]. (K-25)
63-66 Carbide and Carbon Chemicals Co[illegible]p. (Y-12)
67. Columbia University (Dunning)
68-71. General Electric Company, Richland
72. Hanford Operations Office
73-74. Idaho Operations Office
75. Iowa State College
76-79. Knolls Atomic Power Laboratory
80-83. Los Alamos
84. Mallinckrodt Chemical Works
85-87. Mound Laboratory
88. National Advisory Committee for Aeronautics
89. National Bureau of Standards
90. Naval Radiological Defense Laboratory
91. NEPA Project
92. New Brunswick Laboratory
93-96 New York Operations Office
97. North American Aviation, Inc.
98. Patent Branch, Washington
99. Sandia Laboratory
100-114. Technical Information Branch, ORE
115 UCLA Medical Research Laboratory (Warren)
116-120. University of California Radiation Laboratory
121-122 University of Rochester
123-126 Westinghouse

[redacted]

CAUTION

This document [redacted]
Defe[redacted] States. Its [redacted]
disclosure of its [redacted]
pers[redacted]
pen[redacted]

[redacted]

[redacted]

This report is one of a series on shielding and represents part of the work of a summer group working principally at Oak Ridge National Laboratory. Participants are drawn from Nuclear Development Associates (Navy contract), NEPA, Bureau of Ships and Bureau of Aeronautics (Navy Department), AEC, RAND, General Electric, Argonne and Oak Ridge National Laboratory.

These reports are issued through ORNL on Contract No. W-7405, eng. 26.

I. Introduction

Since 1947, a group at ORNL under the direction of E. P. Blizard has been making shielding measurements in the core hole of the Oak Ridge pile shield. Up to the end of 1948, about forty different measurements were made. The results of these tests have been published in the following reports: ORNL-32, ORNL-33, ORNL-159, ORNL-209, ORNL-228, ORNL 435, ORNL-438, C.F. #47-1133, and BNL-C-64.

The object of these different tests varied from studying methods of making attenuation measurements to obtaining engineering information for stationary pile shield designs and fundamental information for mobile reactor design. The purpose of this report is to summarize the neutron data for the most valuable tests of uniform shield where both the shield attenuation and composition are considered well known. Also the results of heavy metal differential neutron measurements will be reported, even though the composition of the neutron analyzer is not well known. In these experiments, measurements were made in a uniform "analyzer" shield with and without a heavy metal front slab. The difference is an index of the fast neutron shielding characteristics of the metal.

II. The Core Hole Facility

The shield testing facility is the core hole through the seven foot Oak Ridge pile shield, at the center of the west face of the pile. The iron-lined hole is $28\frac{1}{2}$" x $32\frac{1}{2}$" at the outside and 24" x 28" at the inside face, with three intervening steps as shown in Fig. 1.

A typical arrangement of shield blocks is shown in the hole. The X pile shield consists of 5' of barytes concrete between two 1' ordinary concrete walls. The asymptotic neutron relaxation length is about 10 cm, nearly the same as for ordinary concrete (ORNL-203).

The Oak Ridge shield is 6' from the pile face, and the core hole is in line with the loading tubes in the graphite. The nearest slugs in the standard pile loading are 74" from the graphite face. The fast neutron flux at the core hole was increased by loading a single slug at the near end of each loading tube, which is visible through the core hole.

The thermal neutron flux incident on the shield sample at a pile power of 3800 KW is 5×10^9 n/cm^2/sec as measured by a silver wire. The gamma flux, extrapolated from ionization chamber readings in ordinary concrete, is about 12000 R/hr. (ORNL-33).

III. Review of Measurement Program

The past shield measurement program may be divided into several distinct phases. The first major phase consisted of engineering type attenuation tests of Brookhaven concrete, Portland concrete, Hanford laminated shielding, and iron -aggregate concrete designed to simulate the Hanford composition. These tests were undertaken to give practical information to aid in the design of stationary pile shields. Most of these tests cannot be considered as useful for fundamental shielding studies since the hydrogen content of the shields was not very well known. The uncertainty was especially great for the tests in which high volume fractions of Portland cement were used to provide the water content, as in the iron-aggregate tests. (Memo from Rockwell to Blizard, Y-El-1, 9/2/49).

Concurrent with these early engineering tests, efforts were made to counter the effect of streaming of neutrons from the surrounding poor X shield into the shield under test. The ratio of neutron relaxation lengths for the two materials was nearly two for most heavy aggregate tests.

The usual method of neutron measurement was to obtain the thermal neutron distribution by irradiation of gold foils, 25 sq. cm in area. Since

most of the shields under test were good moderators, the thermal flux was assumed proportional to the fast flux. In some cases indium foils, bare or cadmium covered, were used.

In an attempt to overcome the effects of streaming, a number of early tests were carried out with 16" shield blocks with spaces between the blocks. It was hoped to match the average neutron attenuation in the X shield by these tactics. Actually the tests measured a laminated air-concrete shield, and showed pronounced evidence of lateral streaming in the air gaps. The neutron streaming was studied by taking horizontal and vertical gold foil traverses at about 8" intervals in the shield blocks.

This type of "laminated" shield test was soon abandoned, and measurements of efficient shields were made only in the outside two or three steps of the core hole. This reduced the magnitude of the streaming problem, because of the initial attenuation of neutrons in the first few feet of the X shield. It was still necessary to measure neutron traverses to determine the effects of streaming. These problems still remain to some extent even with a good shield surrounding the test plug, since there is streaming down the cracks between the sample and the shield. The steps are provided to reduce these effects. In the core hole measurements, both effects were superimposed.

The second phase of the measurement program was still essentially an engineering phase, but the shield compositions were somewhat better controlled. Magnesium oxychloride-iron aggregate shields were developed to compete with and improve on Hanford shield characteristics. The M.O. and M.I. shields were developed and tested. The compositions are given in Table 5. A series of tests with M.O. were made to find the effect of iron and boron containing "thermal" shields on the neutron and gamma attenuation. Finally a differential test, using a uranium converter source of fast neutrons, was used to determine the attenuation of neutrons with a spectrum near that of a fission spectrum.

This technique was also introduced to increase the effective source strength, and decrease the effects of streaming. However, it was too difficult and dangerous to use in subsequent core hole tests.

In the last phase of the core hole program a study of materials and geometrical arrangements potentially useful for mobile reactors was initiated. This involved a study of boron cement and lead, tungsten carbide and boron carbide, and paraffin in various geometries. These measurements were limited by streaming, and by the small range of attenuation measurable with gold foils in boron, except for interesting experiments on boron cement and a laminated $WC-B_4C$ shield. Also, differential experiments to determine the effects of heavy metals on neutrons yielded interesting results. In this phase, slab thicknesses were reduced to one or two inches, in order to obtain more detailed neutron and gamma attenuation information. This improvement was especially dictated because of the sparse gamma attenuation data previously obtained with the large blocks.

Since the core hole dimensions introduced undesirable streaming and geometry problems, and the enforced experimental conditions for gamma measurements were so poor, a better experimental facility was needed. Based on previous experience, a new external lid tank facility was designed by Blizard and Clifford. This facility is described in CRNL-402. The first major experiment undertaken is a measurement of fission neutrons and pile gammas in water through an attenuation of about 10^9.

IV. Summary of Best Measurements in Uniform Shields

This report presents a critical review of the neutron test data to select the best measurements of uniform shields. The criteria for judging the tests are given below:

a. A knowledge of shield composition to within 15%, except for the hydrogen content. Here an uncertainty of ± 15% was considered acceptable, unless the hydrogen content was very low, when a

greater uncertainty was accepted.

b. A measured attenuation over a range of 10^5 or greater, without noticeable interference due to streaming from the X shield.

The criterion for bad streaming has not been rigorously defined, but two aids were used in the selection. First, if there was a noticeable deviation from the exponential or smooth attenuation curve on a logarithmic scale at large thicknesses, together with the obvious effects of streaming present in the traverses, the data would not be considered reliable. Second, if the traverses were sufficiently poor so that the logarithmic extrapolation of the difference between the central foil activity and the side activities amounted to 10% or more of the central reading, the central measurement was rejected. Vertical traverses were always worse than horizontal, because of the larger crack at the top. This was kept in mind in estimating the valid range of attenuation.

The measurements of uniform shields which fall into this strict category are limited to Portland concrete, M.O., M.I. iron aggregate concretes, boron cement, and a laminated $WC-B_4C$ shield. To this list can be added Hill and Roberts' measurement of the attenuation of fission neutrons from a point source in water. These measurements can be converted to the equivalent attenuation for an infinite isotropic plane source, for comparison with the core hole measurements. As will be shown below, the core hole measurements approximate the conditions for an infinite isotropic fission source.

A. <u>M.O. Concrete</u>

M.O. concrete is the high density (5.6 gm/cc) iron aggregate-magnesium oxychloride cement mixture developed to improve on the characteristics of the Hanford and Brookhaven shields. Both the M.O. and Brookhaven shields have about 20 mg. mole/cc of hydrogen, compared to 42 mg mole/cc in the Hanford shield. However, the density of M.O. was increased to 5.6 gm/cc, compared to

4.3 gm/cc for both Hanford and Brookhaven, in order to improve the gamma attenuation characteristics of the shield. This improvement was possible because of the high specific water content of M.O. cement. The mixing and handling characteristics of M.O. concrete are described in ORNL-17, ORNL-240, and ORNL-323.

The most reliable data on M.O. concrete were obtained in runs 30 and 31. In run 30 an array of one inch diameter uranium slugs was buried in a two inch layer of lead in front of the M.O. concrete sample. This uranium plate was designed to convert the thermal neutron flux from the pile into a fast neutron flux from the plate. This arrangement was used to simulate a fission spectrum from a highly enriched small pile. In run 31 a standard core hole-pile source attenuation test was made, with two inches of lead preceding the M.O. concrete.

The attenuation curves in Fig. 2 show that the effective source strength was increased by a factor of ten with the fission source, and that the attenuation characteristics of both the pile spectrum and the modified fission spectrum in M.O. concrete are nearly the same. The characteristics for the source alone are obtained from the difference of the two measurements (Fig. 3). The traverses for the two runs, and the differences, are plotted in Figs. 12, 13, and 14. The traverses for run 30 are better than the corresponding ones for run 31 due to the higher neutron flux in the M.O. shield, with the consequent reduction in streaming from the X shield.

The attenuation for the finite fission source can be converted to the attenuation for the equivalent isotropic infinite, plane source by the method of Welton in LP-141, or by the method of Hurwitz. Following the latter,

[redacted]

$$I(z)_\infty = 2\pi \int_z^\infty R\, f(R)\, dR$$

$$= 2\pi \int_z^{\sqrt{z^2 + a^2}} R\, f(R)\, dR + 2\pi \int_{\sqrt{z^2 + a^2}}^\infty R\, f(R)\, dR$$

$$= I(z) + I(\sqrt{z^2 + a^2}) + I(\sqrt{z^2 + 2a^2}) + \ldots$$

where $I(z)_\infty$ is the required attenuation as a function of z for the infinite plane source, R is the distance from a source point to the measured axial point of coordinate z, a is the radius of the circular source, **I(z) is the measured** attenuation for a finite source **and f(R) is the measurement due to the point source. A table for the pertinent data is given below, (Table I), and the results are plotted in Fig. 3.**

TABLE I

M.O. Thickness (inches)	Run 30 File + Source (cts/min/kw)	Run 31 Pile Only (cts/min/kw)	Finite Source (cts/min/kw)	Infinite Source (cts/min/kw)
0	6.17×10^5	2.52×10^5	3.65×10^5	3.76×10^5
4	2.16×10^5	2.02×10^4	1.96×10^5	2.04×10^5
12	1.11×10^4	8.48×10^2	1.02×10^4	1.10×10^4
20	3.51×10^2	3.08×10^1	3.20×10^2	3.84×10^2
28	1.21×10	1.11×10^0	1.10×10^1	1.34×10^1
36	3.34×10^{-1}	4.22×10^{-2}	2.92×10^{-1}	4.72×10^{-1}
44*	1.26×10^{-2}	0.95×10^{-3}	1.16×10^{-2}	———
λ =	5.9 cm	6.1 cm	5.8 cm	6.0 cm

* streaming

[redacted]

The small change in relaxation length indicates that the corrections were small over the range of attenuation measured. The results also indicate that the corrections are in such a direction that the relaxation length for the typical core hole measurement is very nearly equal to that for an infinite plane fission source.

B. M-1 Concrete

M-1 concrete is a high density (4.7 gm/cc) iron aggregate magnesium-oxychloride cement shield designed to match the Hanford shield approximately in density and hydrogen content, M-1 includes about 1% by weight of boron in the form of colemanite. It was hoped that the addition of boron would reduce the production of hard secondary gamma rays in the shield, so that the gamma performance would compete with the M.O. shield.

The M-1 tests are described in detail in ORNL-438. Two reliable tests of M-1 concrete were made (runs 15 and 46) with somewhat different compositions (Table 5). The actual densities were 4.5 and 4.7 gm/cc respectively. The two attenuation curves are plotted in Fig. 4, together with that for M.O. in run 30. The attenuation for all three tests are nearly exponential with approximately the same relaxation lengths, i.e. 5.8, 5.9, and 6.1 cm. The attenuation data for run 46 are detailed every two inches over a range of 10^4, but do not include traverse data. The traverse data for run 15 are plotted in Fig. 15.

C. Laminated WC-B_4C

One of the measurements of WC and B_4C, supplied by NEPA, very nearly meets the criteria for inclusion in this set of experiments. An attenuation of 10^5 was measured through 40" of laminated WC and B_4C shielding slabs. However, the composition of the first half differed somewhat from the composition in the second half. Since two distinct relaxation lengths were measured, the measurements in the second half are taken as a valid indication of the performance of

that composition. The change in spectrum from the first to the second half is assumed to be small enough so as not to influence significantly the measured relaxation length due to boundary effects. These measurements are reported in detail in ORNL-435. The composition of both halves is given in Table 5. The average density of WC-B_4C components is 5.0 gm/cc in the first half, as compared with 4.2 gm/cc for the second half. The density of the WC is 7.9 gm/cc and of B_4C is 1.9 gm/cc. The average lamination is 2.0" of WC and 3" of B_4C in the second half. Corresponding values are 2" WC, and 2" B_4C for the first half. The reduced densities were used to decrease the weight per slab, and more nearly match the attenuation characteristics of the X shield in order to reduce streaming problems. The WC slabs were sheathed with 1/8" wall aluminum, while the B_4C slabs were covered with 1/16" aluminum. The traverses are plotted in Fig. 16, and the attenuation is given in Fig. 5. Foil measurements were made at the boron tungsten boundaries and the tungsten boron boundaries. The foil activities differ by a factor of 1.2 in these positions, and these activities have been normalized together in Fig. 5.

The attenuation shows a definite change in character at the interface between the two shield compositions. The relaxation lengths are 8.7 cm and 6.5 cm for the first and second halves, respectively. The corresponding mass attenuation factors are 43.5 gm/cm^2 and 27.3 gm/cm^2. These figures assume that the characteristics of the aluminum are not significantly different from those of the WC-B_4C as measured; i.e. the density of the aluminum is assumed to be the same as the WC-B_4C mixture.

The results indicate a striking difference in the neutron characteristics of the two mixtures. If there was no significant interaction of neutron behavior between the boxes, evidently the absorption coefficients for mixtures are not linear combinations of coefficients for the individual materials. This may be expected since the dominant energies are different in the two shields.

D. Water

The most reliable data known for the attenuation of fission spectrum neutrons in water are those of Hill and Roberts (ORNL-181). Measurements have been made in the core hole water tank (ORNL-159), but the influence of streaming limited the reliable attenuation range too severely. Pile neutron attenuation data are now being taken by Clifford in the ORNL lid tank facility to serve as background measurements for fission source measurements. Preliminary measurements with a collimated pile source agree well with the data of Hill and Roberts, in the range from 30 to 90 cm, after an R^2 geometry correction. When the fission source data are available from the lid tank, the present range of attenuation will be extended to about 10^9.

The Hill and Roberts data extend 90 cm from the source over a range of 10^6 attenuation for an equivalent isotropic plane source. This point source attenuation has been converted to isotropic plane attenuation by the usual integration procedure:

$$I(z)_\infty = 2\pi \int_z^\infty R\, f(R)\, dR$$

The original point source data are given in Table 12. The pertinent results for the point-plane transformation are also given. The plane data are plotted in Fig. 6, normalized to the boron cement data at the origin.

The fact that the data for a collimated pile source agrees with the point source data after an R^2 correction confirms the idea that the transport kernel governs the attenuation of fast neutrons in water (first collision source). At the same time it means that part of the attenuation from isotropic plane source is due to the $1/\gamma$ asymptotic behavior of the exponential integral characteristic of the transport kernel. In order to observe the effects of neutron build-up and spectral hardening in water, it is necessary to study the collimated plane

attenuation. A plot of this function in Fig. 8 shows that the attenuation is nearly exponential in this range of attenuation and an asymptotic relaxation length of 8.3 cm can be assigned for water. These results indicate that in the observed range of attenuation, the build-up and hardening effects tend to cancel each other, yielding nearly exponential attenuation.

E. Boron Cement

Boron cement is the hydrogenous component of the M-1 shield. It consists of equal weights of MgO and colemanite, gauged with saturated $Mg\ Cl_2$ solution. The composition is given in Table 5 under "B.C.". It is a neutron moderator with a density of 2.0 gm/cc and a hydrogen content 0.7 that of water. The oxygen content is 1.2 times that of water, and 8 mg mole/cc of boron are included to reduce secondary gamma production in hydrogen and chlorine.

The boron cement tests were made with 1 inch thick samples behind 2" of lead, used for protection of personnel from pile gammas. The traverses, given in Fig. 17, indicate that streaming becomes serious after about 10^6 attenuation. The attenuation in Fig. 6 exhibits a curvature with a continually increasing "relaxation length." This behavior is similar to water in this respect.

Since the boron cement contains 0.7 gm/cc of water equivalent, the transport kernel is also assumed to be controlling for fast neutron diffusion. In Fig. 7 the isotropic attenuation is multiplied by thickness in inches to approximate the transformation from exponential integral to exponential. The result indicates an asymptotic relaxation length of 7.6 cm. The effect of the front 2" layer of lead in the boron cement test is to increase slightly the initial rate of attenuation over that for no lead.

F. Portland Concrete

Measurements with two different Portland concrete samples were made. (Runs 10 and 29). The composition of each batch was specified as the standard concrete "wall mix"; four parts Tennessee limestone gravel, two parts river sand, and one part Portland cement.

The expected composition of this mix is given in Table 5. The hydrogen concentration is the principal uncertainty. This will vary with the age of the concrete, the external humidity, and the conditions of curing, so that the hydrogen content can be specified only to ± 20%. However, since the volume fraction of cement, and the resulting hydrogen content are both low, this measurement still falls within our category of a "known" composition. From a study of the composition in Table 5, it is seen that Portland concrete is nearly pure oxygen (71.8 mg. atoms/cc vs. 55.5 for H_2O.). The traverses for runs 10 and 29 are given in Fig. 18 and 19. These traverses indicate that attenuations of the order of 10^7 - 10^8 are obtained before streaming becomes objectionable. This is to be expected since Portland concrete is found to have a relaxation length nearly equal to that of the surrounding X shield. The range of valid attenuation in run 10 was limited primarily because of the streaming caused by a 4" air gap following 60" of shielding. This condition was corrected in run 29. The attenuation curves for these two runs are given in Fig. 7. The attenuation exhibits a curvature characteristic of an isotropic plane source and moderating shields containing no heavy metals. At attenuations of the order of 10^5 the rate of attenuation is only slowly varying, and asymptotic relaxation lengths are 10.7 and 10.0 cm for runs 10 and 29, respectively. The average of the two results is 10.35 ± 0.3 cm for concrete of density 2.3 gm/cc. The different attenuation curves may be due to a difference in the water content of the two samples.

If an operation similar to that for B.C. is used to convert the isotropic plane attenuation to the collimated plane case, assuming a transport kernel, the asymptotic character of the attenuations are somewhat more clear. On this basis the relaxation lengths are **11.4** and 10.8 cm respectively, or an average of **11.1 cm.**

G. Review of Uniform Shield Data

The attenuation information on the uniform shields is summarized in the table below. The asymptotic relaxation lengths for the "equilibrium" spectra are given for the appropriate geometries. The results for comparable runs indicate that the shields may be ranked in the following order, neglecting the effects of the different types of diffusion kernels assumed.

Table 2

Shield	Density (gm/cc)	Relaxation Length cm	Relaxation Length gm/cm^2	Plane Geometry
B_4C - WC	6.2	4.7	29	isotropic
M.1.	4.7	5.9	28	"
M.O.	5.6	6.1	34	"
Brookhaven	4.3	6.3	27	"
W-1	3.6	6.6	24	"
Boron Cement	2.0	7.6	15.2	collimated
Water	1.0	8.3	8.3	"
Portland Concrete	2.3	11.1	26	"

The hydrogen concentrations are known to only ± 15% or better on those shields studied in detail (except M-1 - run 15) because these tests were made in the early engineering phase of the program, and were not intended for fundamental measurements. The attenuation characteristics for Brookhaven and W-1 concretes, (Portland cement - iron aggregate shields) are included in the summary because the hydrogen contents are known nearly as well, ± 20%. These show the same general exponential attenuation curves as for the other heavy uniform shields.

V. Differential Slab Experiments

A number of experiments were performed which can be classified as differential slab experiments. In these cases two experiments were made with a given shielding material, which included M.O., B_4C and boron cement. The measurements were made with and without a slab of heavy material in front of the uniform shield. By examining the two attenuation curves, the effect of the heavy slab on the incident neutron spectrum is evident.

In general the spectrum is softened, due primarily to inelastic scattering in the metal. This is evident from the increased rate of attenuation in the early regions of the uniform shield, compared to the attenuation without the heavy slab. At greater thicknesses, the relaxation length approaches that for the test without the slab. In this latter region a characteristic ratio or attenuation factor may be obtained from the two tests. If the attenuation produced by the heavy slab is assumed to be exponential, an effective relaxation length may be determined from the attenuation factor and thickness of the heavy material. It would have been desirable to measure the attenuation as a function of both the thickness of the heavy slab and of the analyzer material to determine the validity of the exponential assumption.

Only a few of the total number of experiments fall into this category. Some which might have been used were designed primarily to find the effect of generation of capture and inelastic scattering gammas in the heavy layer. For this purpose experiments were performed with and without boron layers present. These arrangements complicated the tests so that no direct differential analyses for neutrons could be made. The presence of these extraneous layers will be noted below.

Differential experiments were performed with Fe, WC and Pb in conjunction with M.O., B_4C and boron cement analyzers, respectively. The Fe test compared 2"

[redacted]

of colemanite and M.O. concrete preceded by 1" of B_2O_3 and 7.5" of Fe. The WC test compared "B_4C" preceded by 8.25" of WC (ρ = 7.9 gm/cc), 0.75" of masonite, and 1" of aluminum. For purposes of comparison, the masonite and aluminum were considered equivalent to WC of density 7.9. The Pb test compared 2" of Pb followed by boron cement with 10" of Pb in the same arrangement.

The attenuation data for the various tests are given in Tables 16, 17, 18, and the corresponding curves are plotted in Figs. 9, 10, 11. The pertinent results for the tests are tabulated below. The accuracy of the experiments was insufficient to demonstrate the relative efficiency of lead and iron. However, since the WC was used in only half density, its superiority is clearly demonstrated.

Table 3

Differential Front Slab Experiments

Front Slab	Thickness (inches)	ρ (gm/cc)	Analyzer	Attenuation Factor	"λ" cm
Fe + B_2O_3	7.5" / 1"	7.85 / 1	M.O.	18 ± 3	7.5 ± 0.5
Pb	8"	11.3	B.C.	13 ± 3	8.0 ± 1
"WC"	10"	7.9	"B_4C"	19 ± 2	8.6 ± 0.5

Table 4. Summary of Neutron Characteristics for Uniform Shields

Shield Material	Run No.	Density (gm/cc)	Attenuation Range	Relaxation Length λ(cm)	Relaxation Length $\rho\lambda$ (gm/cm^2)	Reference ORNL Report
*M.O. Concrete	30	5.6	10^7	6.0	34	436
" "	31	5.6	10^6	6.1	34	436
*M.1 Concrete	15	4.5	10^6	5.8	26	438
" "	46	4.7	10^4	5.9	28	438
Brookhaven	3	4.3	10^5	6.3	27	436
Concrete	4	4.3	10^5	6.3	27	436
W.1 Concrete	11	3.6	10^6	6.6	24	209
*WC-B_4C	42	5.0	10^3	8.6	42	435
*B_4C-WC	42	4.2	10^5	7.0	29	435
** Water	H&R	1.0	10^6	8.3	8.3	181
** Boron Cement	34	2.0	10^6	7.6	15.2	436
** Portland Concrete	10	2.33	10^8	11.4	27	209
	29	2.33	10^9	10.8	25	436

Notes:

* "Asymptotic" relaxation length for an isotropic plane source. If a diffusion kernel is assumed λ will be the same for both isotropic and collimated plane sources.

** "Asymptotic" relaxation length for a collimated plane source with a transport kernel assumed.

Table 5. Shield Compositions*

Shield Material	Run No.	Density gm/cc	Elemental Components - (milligram atoms/cc)													
			Fe	H	B	O	Mg	Cl	Ca	Si	Al	Mn	S	C	W	Total
M.O.	30-31	5.6	88.3	26.3(±15%)	--	21.1	8.69	2.05	--	--	--	0.37	--	--	--	146.8
M.I.	15	4.5	55.7	63(±5%)	3.76	47.3	10.5	3.21	1.25	--	--	0.25	--	--	--	187.0
M.I.	46	4.8	68.5	35.9(±20%)	3.91	32.0	8.5	2.89	1.29	--	--	0.28	--	--	--	153.2
Brookhaven	3-4	4.3	54.7	21.1(±20%)	--	47.7	0.35	--	6.45	2.10	0.79	1.22	0.11	--	--	134.5
W1 Concrete	11	3.6	40.5	20.1	3.28	38.8	0.62	--	12.15	3.65	1.36	0.21	0.18	--	--	120.8
WC-B_4C	42	5.0	--	--	62.0	--	--	--	--	--	8.4	--	--	34.2	18.7	123.3
B_4C-WC	42	4.2	--	--	73.6	--	--	--	--	--	7.7	--	--	33.8	14.2	134.3
H_2O	I R	1.0	--	111.0	--	55.5	--	--	--	--	--	--	--	--	--	166.5
Boron Cement	33-34	2.0	--	79.1(±5%)	7.98	68.2	16.42	6.93	2.66							181.3
Portland Cement	18-29	2.33	0.13	4.76(±20%)	--	71.8	0.2	--	14.5	1.56	0.44	--	.06	10.8	--	104.3
WC	37	7.9	--	5.6(±10%)	--	2.8	--	--	--	--	10	--	--	36.7	33.3	88.4
B_4C	36-37	1.9	--	7.2(±10%)	117.5	3.6	--	--	--	--	4.9	--	--	33.7	--	166.9
Hanford W	--	4.3	64.3	42.3(±10%)	--	21.7	--	--	--	--	--	.19	--	26.5	--	154.7

* Based on values given in Conf. Mem. T-El-1 from Rockwell to Blizard, dated 9/2/49

[redacted]

Table 6

Run 30 - Traverses

2" Converter Plate
+ M.O. Concrete
(Pile + Fission Source)

Saturated Activity (cts/min/kw)

Thickness (in. M.O.)	Inches from center							X Factor
	-12	-8	-4	0	4	8	12	
* -2	2.39	2.50	2.60	2.76	2.60	2.48	2.26	($x10^6$)
* 0	5.81	6.01	6.03	6.17	6.01	5.51	5.72	($x10^5$)
* 4	1.18	1.80	2.10	2.16	2.03	1.80	1.22	($x10^5$)
12		0.90	1.11	1.11	0.98	0.75		(10^4)
* 20	3.00	3.28	3.47	3.51	3.14	2.72	2.59	($x10^2$)
28	2.44	1.53	1.25	1.21	1.15	1.08	1.20	(x10)
* 36	6.53	3.97	3.48	3.34	3.14	3.58	10.1	($x10^{-1}$)
44	32.2	9.56	1.89	1.26	1.54	2.01	7.36	($x10^{-2}$)

* Horizontal Traverses

Table 7

Run 31 - Traverses

2" Pb + M.O. Concrete
(Pile Source)

Saturated Activity (cts/min/kw)

Thickness (in. M.O.)	Inches from center							X Factor
	-12	-8	-4	0	4	8	12	
* -2	1.92	2.17	2.18	2.23	2.18	2.26	2.03	($x10^6$)
* 0	1.57	1.84	2.66	2.52	2.02	2.18	2.95	($x10^5$)
* 4	1.32	1.72	1.95	2.02	1.84	1.71	1.41	($x10^4$)
12	- -	7.89	8.83	8.48	7.37	5.92	- -	($x10^2$)
* 20	3.42	3.06	3.11	3.08	2.70	2.58	2.98	(x10)
28	3.20	1.73	1.22	1.11	1.06	1.15	1.85	(x1)
* 36	9.20	6.03	4.62	4.22	4.53	6.31	19.0	($x10^{-2}$)
44	22.6	3.97	0.95	0.95	1.40	11.6	53.1	($x10^{-3}$)

* Horizontal Traverses

Table 8

Differential Experiment

Run 30 - Run 31

Fission Source Only
M.O. Concrete

Saturated Activity (cts/min/KW)

Thickness (in. M.O.)	Inches from center							X Factor
	-12	-8	-4	0	4	8	12	
-2	0.47	0.33	0.42	0.53	0.42	0.22	0.23	($x10^6$)
0	4.24	4.17	3.37	3.65	3.99	3.33	2.77	($x10^5$)
4	1.05	1.63	1.90	1.96	1.85	1.63	1.08	($x10^5$)
12		0.82	1.02	1.02	0.91	0.69		($x10^4$)
20	2.66	2.97	3.16	3.20	2.87	2.46	2.29	($x10^2$)
28	2.12	1.36	1.13	1.10	1.04	0.97	1.01	(x10)
36	5.61	3.37	3.02	2.92	2.79	2.95	8.2	($x10^{-1}$)
44	29.9	9.16	1.79	1.16	1.40	1.89	2.05	($x10^{-2}$)

Table 9

Run 19 - Traverses

M-1 Concrete (ρ = 4.5 gm/cc)
(Au Foils on Wooden Dowels)

Saturated Activity (cts/min/kw)

Thickness (inches)	(Up, Left) - 12	- 8	- 4	Inches From Center 0	- 4	- 8	(Down, Right) - 12	x Facto
* 5	8.03	9.50	10.8	12.1	11.0	9.30	8.20	(x10^3
15		1.44	1.26	1.38	1.27	1.15		(x10^2
*29	12.2	4.07	3.08	3.20	3.33		17.0	(x10$^-$
39	57.5	9.80	2.13	1.11	1.08		12.9	(x10$^-$
				Inserts				
2				2.38				(x10^4
18				1.76				(x10
22				3.59				(x 1
42				Background				

* Horizontal (Alternate with Vertical)

Table 10

Run 46

M-1 Concrete (ρ = 4.7 gm/cc)
(Au Foils on Al Strips)

Thickness (inches)	Sat. Activity (cts/min/kw)	Thickness (inches)	Sat. Activity (cts/min/kw)
0	2.66×10^4	12	1.32×10^2
2	1.08×10^4	14	5.23×10
4	4.74×10^3	16	2.18×10
6	1.81×10^3	18	9.35
8	7.20×10^2	20	4.18
10	3.18×10^2	22	3.02

Table 11

Run 42 - Traverses

Laminated WC - B_4C
(Au Foils on Al Strips)

Saturated Activity (cts/min/kw)

Horizontal Traverses

Thickness	(left)				Inches From Center				(right)	x
(inches)	- 13	- 11	- 8	- 4	0	4	8	11	13	Factor
4.5	4.29	3.02	3.10	3.44	3.59	3.50	3.26	3.21	4.50	($x10^2$)
13.4	2.91	2.16	2.38	2.62	2.70	2.58	2.36	2.32	3.66	(x10)
18.0	7.21	5.44	5.62	6.33	6.66	6.50	5.97	6.01	9.75	(x 1)
25.5	14.9	4.1	3.5	3.7	3.8	3.8	3.6	3.8	9.1	($x10^{-1}$)
32.4	26.5	7.4	4.5	4.4	4.4	4.5	4.2	6.0	19.0	($x10^{-2}$)
40.2	2.3	1.3	1.0	1.0	1.0	1.2	1.2	1.3	1.7	($x10^{-2}$)

Vertical Traverses

Thickness	(top)				Inches from Center				(bottom)	x
(inches)		- 11	- 8	- 4	0	4	8	11		Factor
4.5		5.80	3.41	3.51	3.59	3.34	3.01	3.65		($x10^2$)
13.4		3.37	2.49	2.65	2.70	2.52	2.21	2.53		(x10)
18.0		9.55	6.21	6.40	6.66	6.35	5.68	6.39		(x 1)
25.5		12.3	4.0	3.8	3.8	3.7	3.5	8.6		($x10^{-1}$)
32.4		4.11	6.4	4.5	4.4	4.3	4.7	16.1		($x10^{-2}$)
40.2		6.1	2.2	1.1	1.0	1.1	1.0	1.3		($x10^{-2}$)

Table 12

Fission Source Water Attenuation

Hill and Roberts Experiment *

R cm	A_γ cts/m	RA_γ cm cts/min	ΣRA_γ cm^2 cts/min	R in
10	1.40×10^{3}	1.40×10^{4}	4.09×10^{4}	3.9
20	8.13×10^{1}	1.63×10^{3}	3.23×10^{3}	7.9
30	8.32×10^{0}	2.50×10^{2}	9.26×10^{2}	11.8
40	1.30×10^{0}	5.20×10^{1}	2.00×10^{2}	15.8
50	2.26×10^{-1}	1.13×10^{1}	4.53×10^{1}	19.7
60	4.42×10^{-2}	2.65×10^{0}	1.10×10^{1}	23.7
70	9.44×10^{-3}	6.61×10^{-1}	2.92×10^{0}	27.6
80	2.29×10^{-3}	1.83×10^{-1}	8.28×10^{-1}	31.5
90	5.82×10^{-4}	5.24×10^{-2}	2.38×10^{-1}	35.5

*Taken from smoothed data of Table IV, ORNL-181

Table 13

Run 34 - Traverses

2" Pb + Boron Cement
(Au Foils on Al Strips)

11" B. C. Traverse

Horizontal

(in)	(cts/min/kw)
- 12	28.3
- 8	23.1
- 4	25.1
0	27.3
+ 4	25.4
+ 8	26.3
+ 12	33.1

Vertical

(in)	(cts/min/kw)
- 10.5	45.6
- 7.0	27.8
- 3.5	27.4
0	27.3
+ 3.5	25.0
+ 7.0	22.8
+ 10.5	27.9

23" B. C. Traverse

- 13.5	0.837
- 9.0	0.412
- 4.5	0.398
0	0.376
+ 4.5	0.341
+ 9.0	0.353
+ 13.5	0.643

- 12	1.45
- 8	0.546
- 4	0.425
0	0.376
+ 4	0.353
+ 8	0.346
+ 12	0.602

29" B. C. Traverse

- 13.5	6.70×10^{-2}
- 9.0	2.70×10^{-2}
- 4.5	2.37×10^{-2}
0	1.94×10^{-2}
+ 4.5	1.79×10^{-2}
+ 9.0	1.98×10^{-2}
+ 13.5	5.14×10^{-2}

- 12	14.8×10^{-2}
- 8	3.36×10^{-2}
- 4	1.95×10^{-2}
0	1.94×10^{-2}
+ 4	1.82×10^{-2}
+ 8	1.98×10^{-2}
+ 12	5.14×10^{-2}

Table 14 Run 10 - Traverses

Portland Concrete
(Au Foils on Wooden Dowels)

Saturated Activity (cts/min/kw)

Thickness (inches)	(Up, Left) - 12	- 8	- 4	Inches From Center 0	4	8	(Down, Right) 12	x Factor
* 8	1.77	2.52	2.91	2.96	2.88	2.42	1.41	($x10^5$)
16		1.24		1.22		1.25		($x10^4$)
*25			8.05	7.68	8.35			($x10^2$)
35		7.59	5.79	5.16		8.49		(x 10)
*45		6.59	4.36	5.03	5.66	7.19	8.38	(x1)
55	1.17	9.91	5.98	4.42	3.90	5.16	4.57	($x10^{-1}$)
*66	6.54	6.97	5.61	5.03	4.43	4.64	4.90	($x10^{-2}$)
78	2.41			1.92			15.3	($x10^{-3}$)

*Horizontal (Alternate with Vertical)

Table 15 Run 29 - Traverses

Portland Concrete
(Au Foils on Wooden Dowels)

Saturated Activity (cts/min/kw)

Thickness (inches)	(Up, Left) - 12	- 8	- 4	Inches From Center 0	4	8	(Down, Right) 12	x Factor
* 8	0.682	1.30	1.56	1.64	1.65	1.47	0.778	($x10^6$)
16		10.0	10.4	9.82	9.42	7.83		($x10^3$)
*25	5.19	5.42	4.96	4.67	5.02	5.33	5.33	($x10^2$)
35		3.54	3.10	2.74	2.77	3.02		(x10)
*49	9.28	8.69	7.50	7.42	8.05	9.17	10.1	($x10^{-1}$)
59	1.57	1.32	8.82	6.02	5.93	7.52	6.82	($x10^{-2}$)
*66	3.37	2.08	1.39	1.13	1.52	1.80	2.61	($x10^{-2}$)
78	11.2	5.09	2.45	1.35	1.15	1.52	2.29	($x10^{-3}$)

Table 16

Differential Front Slab Experiment
Iron Slab
M.O. Concrete Analyzer
(Au foils on wooden dowels)

Thickness of M.O. (inches)	Run 23 Sat. Activity (cts/min/KW)	Run 25 Sat. Activity (cts/min/KW)
4	5.32×10^{2}	8.57×10^{1}
12	3.37×10^{1}	2.52×10^{0}
20	1.91×10^{0}	9.81×10^{-2}
28	9.41×10^{-2}	5.07×10^{-3}
36	3.23×10^{-3}	1.0×10^{-4}

Table 17

Differential Front Slab Experiment
Lead Slab
Boron Cement Analyzer
(Au foils on Al strips)

Boron Cement Thickness (inches)	Run 34 Sat. Activity (cts/min/KW)	Run 23 Sat. Activity cts/min/KW)
0	2.51×10^{5}	- - - -
1	9.42×10^{3}	2.38×10^{3}
3	2.54×10^{3}	6.15×10^{2}
5	6.19×10^{2}	1.28×10^{2}
7	2.04×10^{2}	3.37×10^{1}
9	7.48×10^{1}	1.02×10^{1}
11	2.72×10^{1}	2.97×10^{0}
13	1.19×10^{1}	1.14×10^{0}
15	4.42×10^{0}	4.22×10^{-1}
17	1.99×10^{0}	1.80×10^{-1}
19	8.70×10^{-1}	6.31×10^{-2}
21	3.76×10^{-1}	3.25×10^{-2}
23	1.63×10^{-1}	1.57×10^{-2}
25	8.12×10^{-2}	6.34×10^{-3}
27	3.95×10^{-2}	3.72×10^{-3}
29	1.94×10^{-2}	3.03×10^{-3}
31	1.67×10^{-2}	2.18×10^{-3}
33	9.24×10^{-3}	6.88×10^{-3}

Run 23: + 2" Colemanite + M.O. Concrete
Run 25: 1" B_2O_3 + 7.5" Fe + 2" Cole. + M.O. Concrete

Run 34: 2" Pb + Boron Cement
Run 33: 10" Pb + Boron Cement

Table 18

Differential Front Slab Experiment
"WC" Slab
"B_4C" Analyzer

Au foils on 1/4" Masonite
Run 36 *
B_4C + Al + Masonite

(inches)	(c/m/KW)
2.88	737
5.25	267
7.63	106
10.00	44.7
12.4	20.7
14.8	14.0
21.4	0.99

Au foils on Al strips
Run 39
B_4C + Al

(inches)	(c/m/KW)
2.38	370
4.50	137
6.62	66.0
8.75	32.6
10.9	15.0
13.0	7.0

Run 37 **
WC + Al + Masonite (10")

(inches)	(c/m/KW)
5.00	49.2
7.42	13.3
9.75	3.92
12.12	1.40
21.35	0.054

Run 40 ***
WC + Al (9.25")

(inches)	(c/m/KW)
2.37	188
4.50	41.0
6.63	11.8
8.75	4.19
10.87	1.41
13.00	3.10

* Composition: See Table 5

** 8.25" WC + 1" Al + 0.75" Masonite

*** 8.25" WC + 1" Al

[redacted]

Dr. 7851

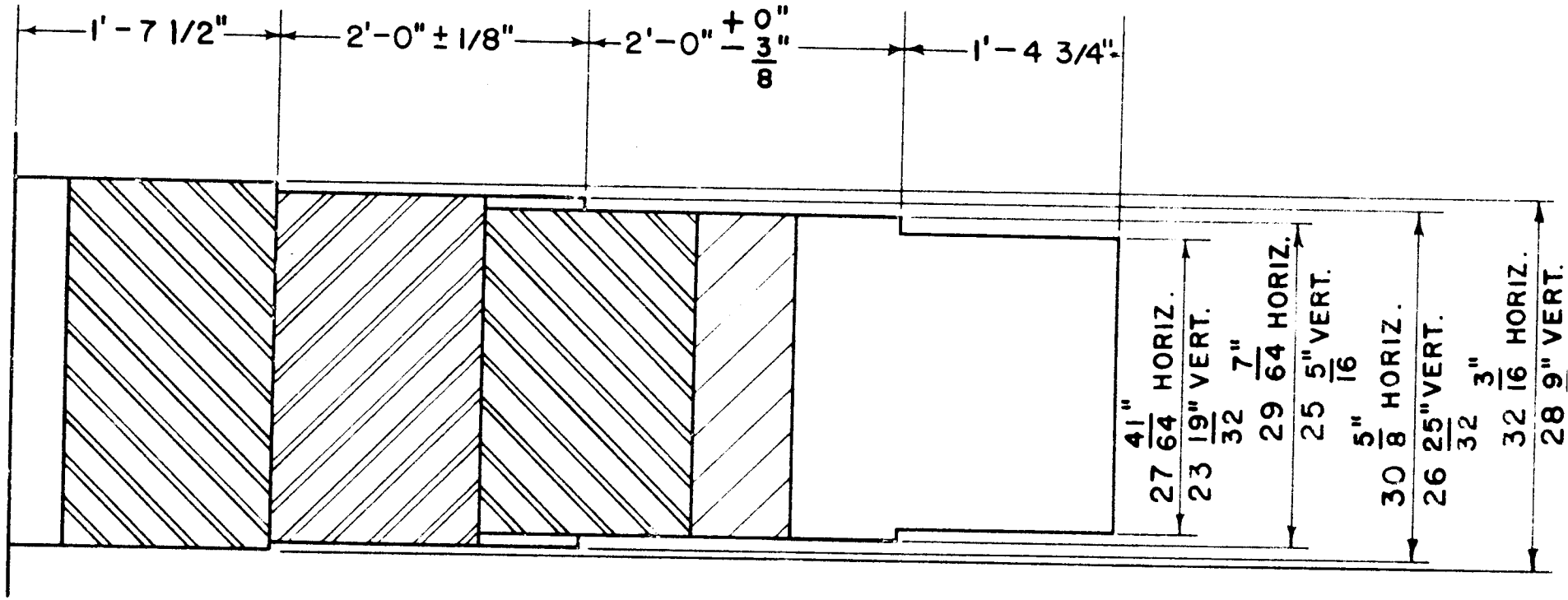

CORE HOLE
FIG. 1 PAGE 30

FIG. 2 PAGE 31

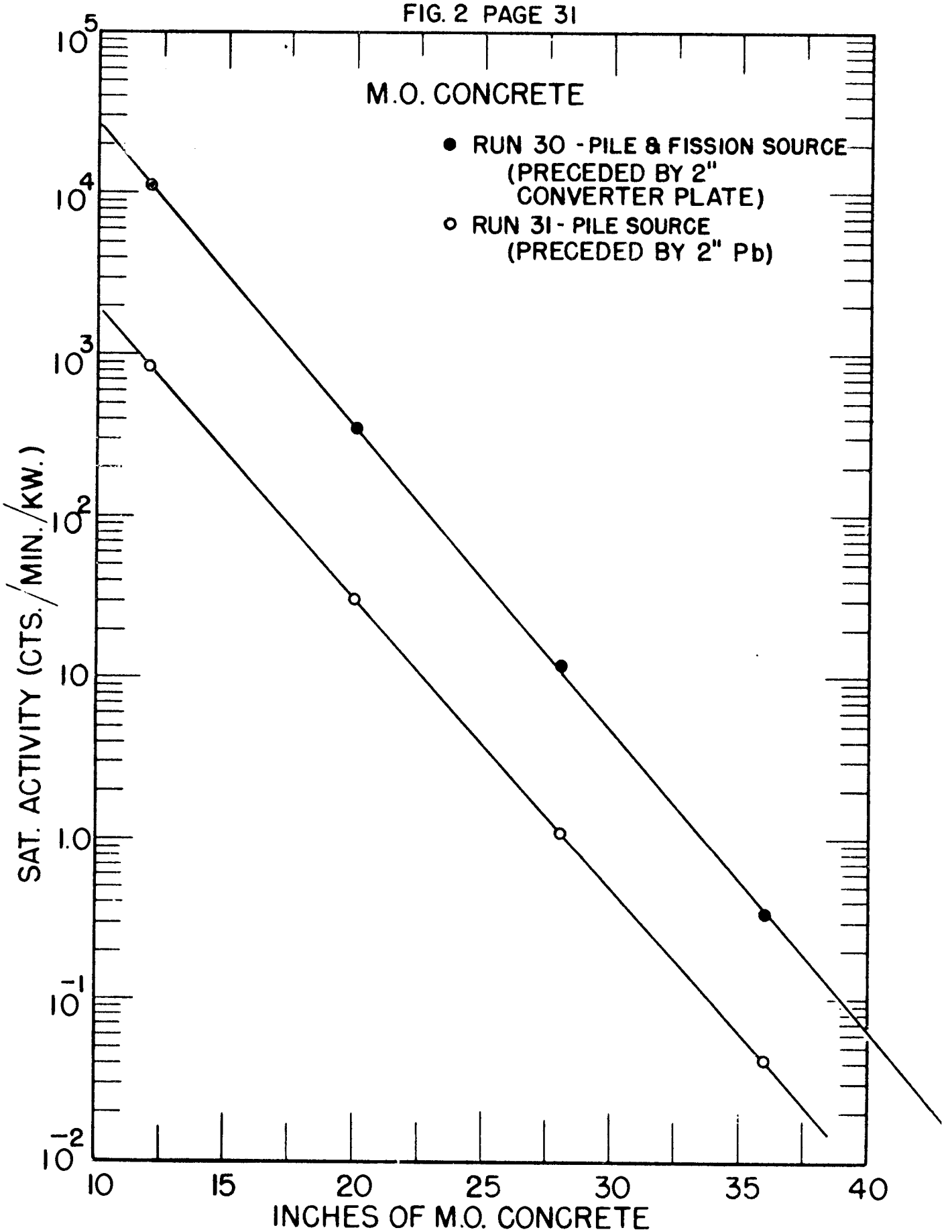
M.O. CONCRETE
● RUN 30 - PILE & FISSION SOURCE (PRECEDED BY 2" CONVERTER PLATE)
○ RUN 31 - PILE SOURCE (PRECEDED BY 2" Pb)
SAT. ACTIVITY (CTS./MIN./KW.)
10^5
10^4
10^3
10^2
10
1.0
10^{-1}
10^{-2}
10
15
20
25
30
35
40
INCHES OF M.O. CONCRETE

FIG. 3 PAGE 32

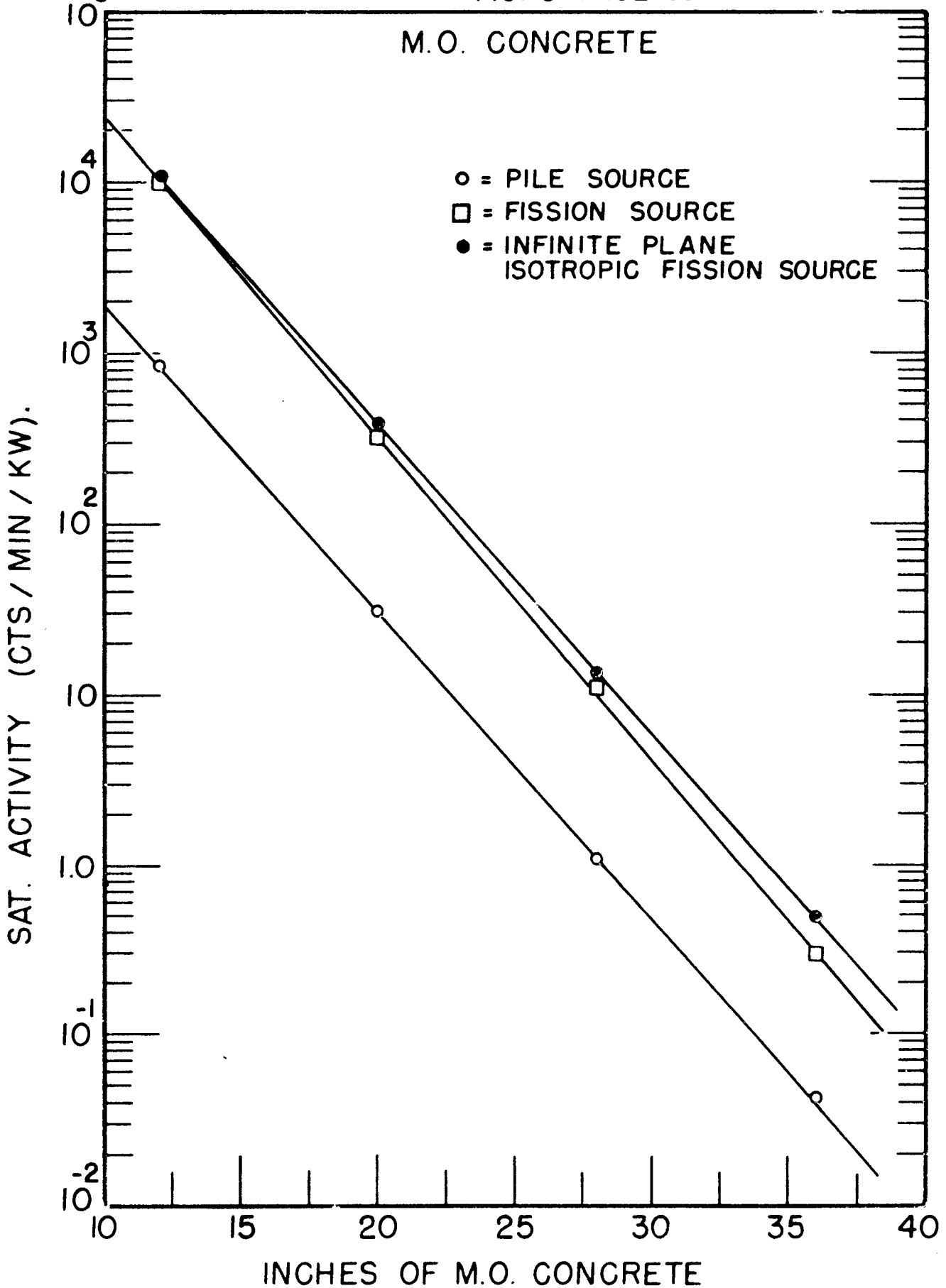
M.O. CONCRETE
o = PILE SOURCE
□ = FISSION SOURCE
● = INFINITE PLANE ISOTROPIC FISSION SOURCE
SAT. ACTIVITY (CTS / MIN / KW).
10^5
10^4
10^3
10^2
10
1.0
10^{-1}
10^{-2}
10
15
20
25
30
35
40
INCHES OF M.O. CONCRETE

FIG. 4 PAGE 33

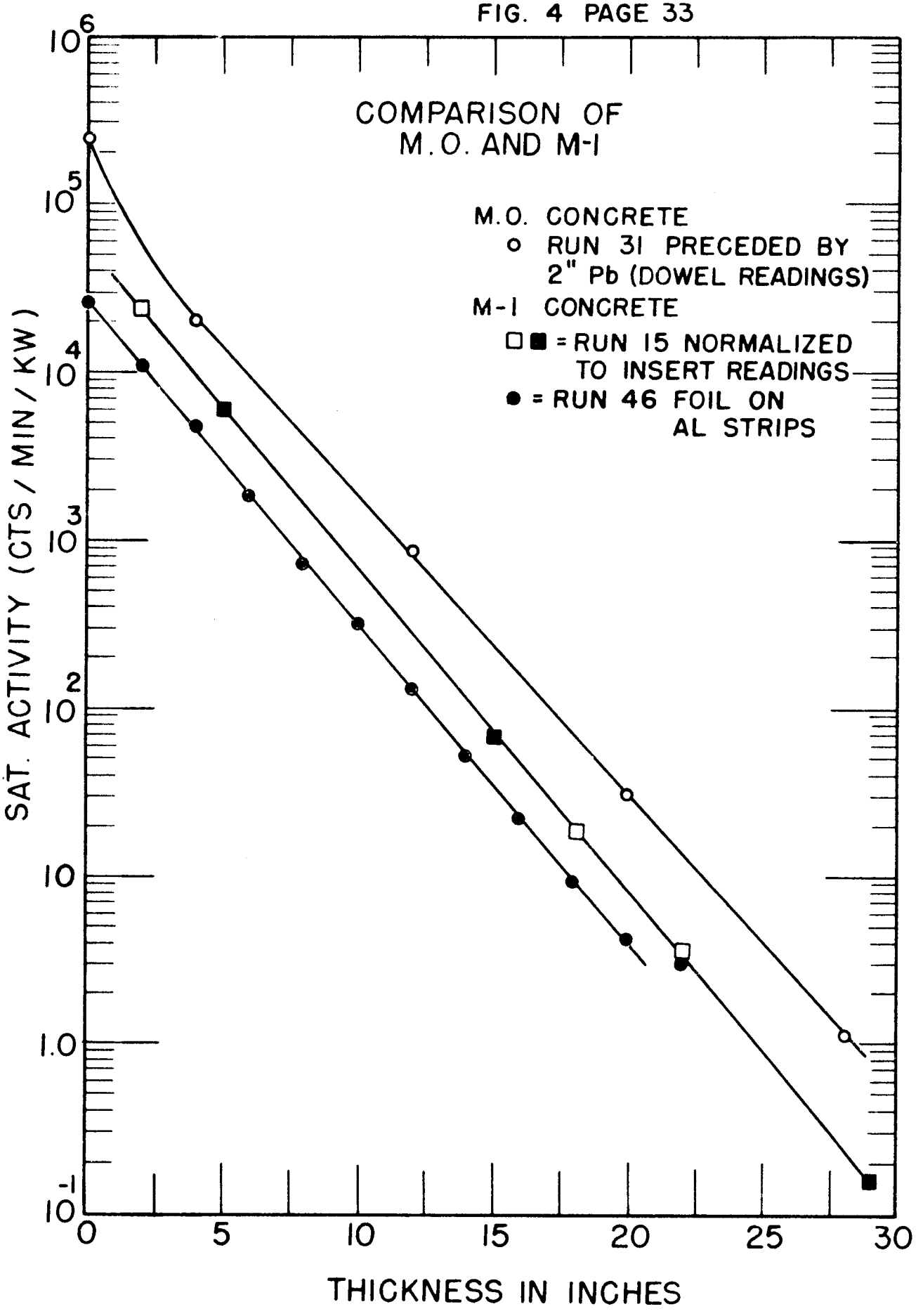
COMPARISON OF
M.O. AND M-I
M.O. CONCRETE
○ RUN 31 PRECEDED BY 2" Pb (DOWEL READINGS)
M-I CONCRETE
□ ■ = RUN 15 NORMALIZED TO INSERT READINGS
● = RUN 46 FOIL ON AL STRIPS
SAT. ACTIVITY (CTS / MIN / KW)
10^6
10^5
10^4
10^3
10^2
10
1.0
10^{-1}
0
5
10
15
20
25
30
THICKNESS IN INCHES

FIG. 5 PAGE 34

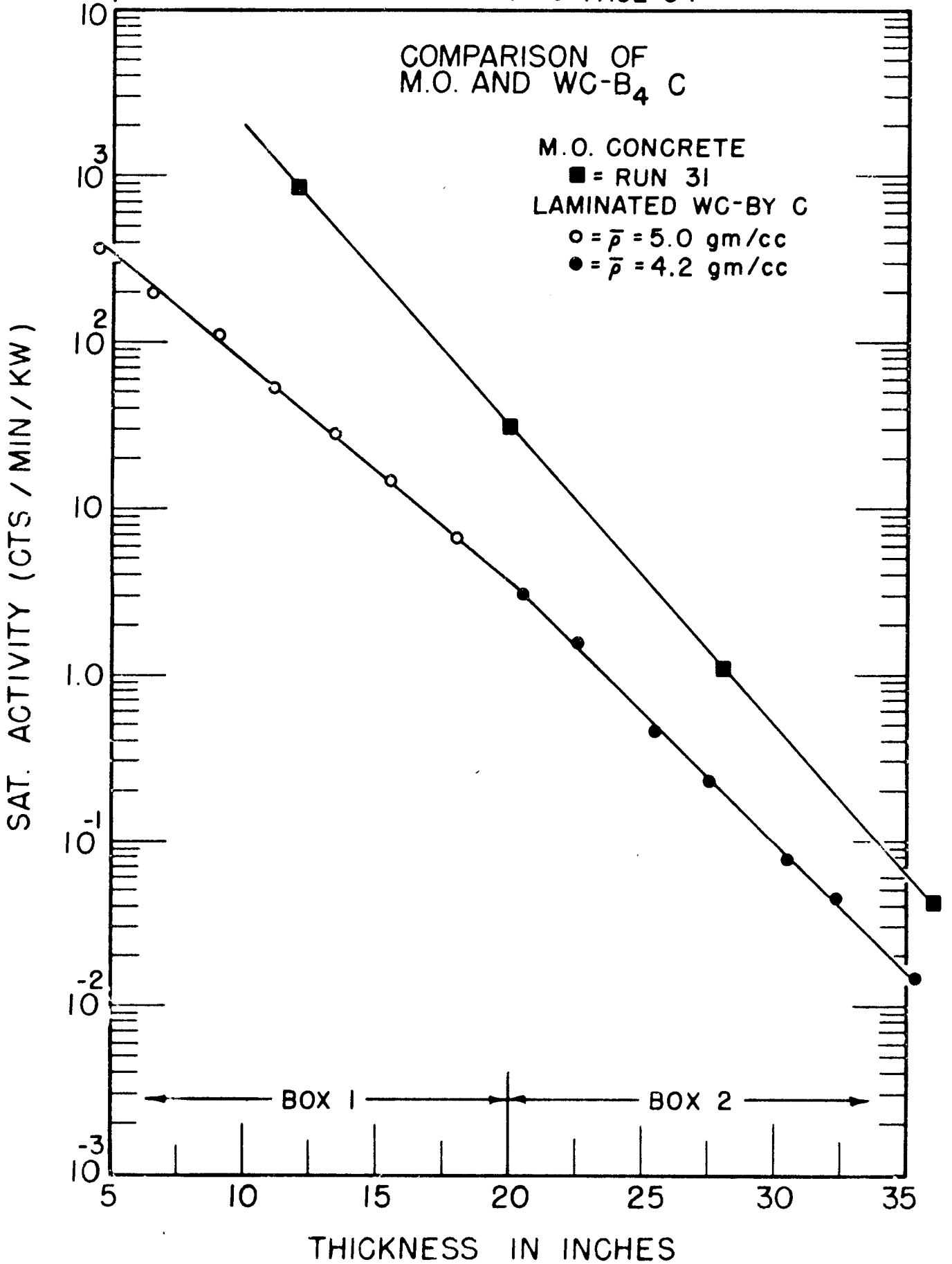
COMPARISON OF
M.O. AND WC-B4 C
M.O. CONCRETE
■ = RUN 31
LAMINATED WC-BY C
○ = ρ̄ = 5.0 gm/cc
● = ρ̄ = 4.2 gm/cc
SAT. ACTIVITY (CTS / MIN / KW)
10^4
10^3
10^2
10
1.0
10^-1
10^-2
10^-3
BOX 1
BOX 2
5
10
15
20
25
30
35
THICKNESS IN INCHES

FIG. 6 PAGE 35

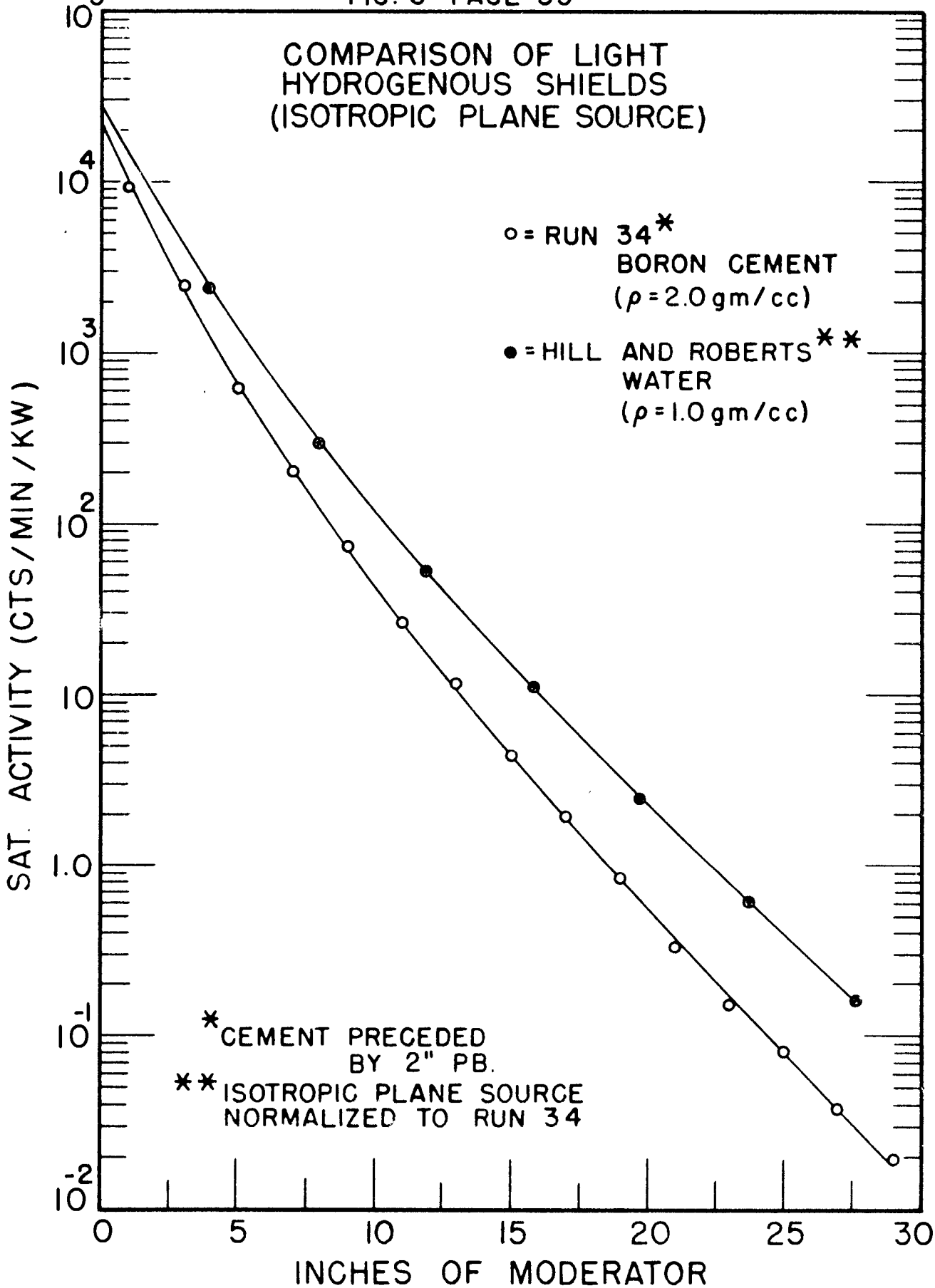
COMPARISON OF LIGHT
HYDROGENOUS SHIELDS
(ISOTROPIC PLANE SOURCE)
o = RUN 34*
BORON CEMENT
(ρ = 2.0 gm/cc)
● = HILL AND ROBERTS**
WATER
(ρ = 1.0 gm/cc)
*CEMENT PRECEDED
BY 2" PB.
**ISOTROPIC PLANE SOURCE
NORMALIZED TO RUN 34
SAT. ACTIVITY (CTS/MIN/KW)
INCHES OF MODERATOR
10^5
10^4
10^3
10^2
10
1.0
10^{-1}
10^{-2}
0
5
10
15
20
25
30

FIG. 7 PAGE 36

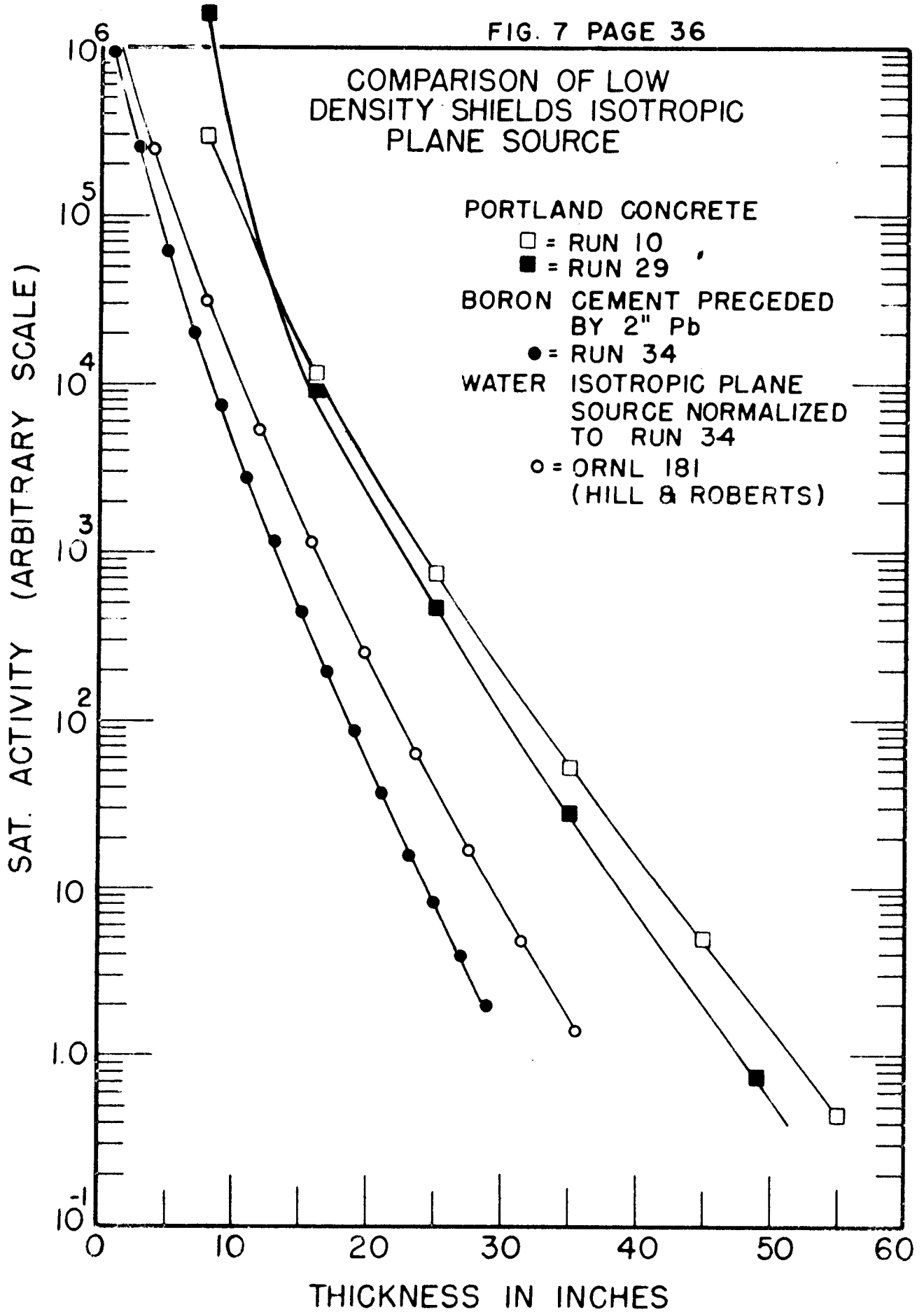
COMPARISON OF LOW DENSITY SHIELDS ISOTROPIC PLANE SOURCE
PORTLAND CONCRETE
□ = RUN 10
■ = RUN 29
BORON CEMENT PRECEDED BY 2" Pb
● = RUN 34
WATER ISOTROPIC PLANE SOURCE NORMALIZED TO RUN 34
○ = ORNL 181 (HILL & ROBERTS)
SAT. ACTIVITY (ARBITRARY SCALE)
10^6
10^5
10^4
10^3
10^2
10
1.0
10^{-1}
0
10
20
30
40
50
60
THICKNESS IN INCHES

FIG. 8 PAGE 37

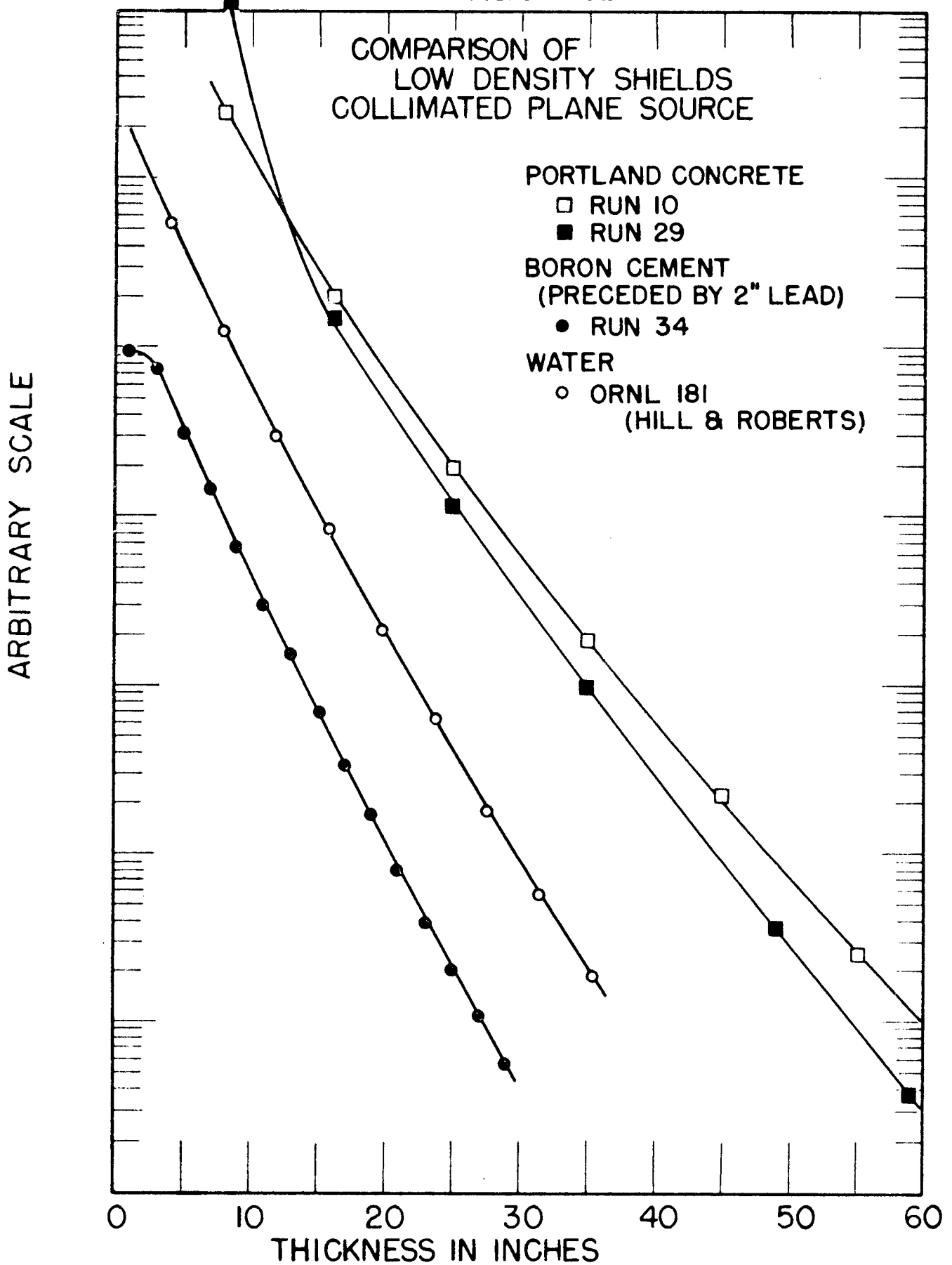
COMPARISON OF
LOW DENSITY SHIELDS
COLLIMATED PLANE SOURCE
PORTLAND CONCRETE
RUN 10
RUN 29
BORON CEMENT
(PRECEDED BY 2" LEAD)
RUN 34
WATER
ORNL 181
(HILL & ROBERTS)
ARBITRARY SCALE
0
10
20
30
40
50
60
THICKNESS IN INCHES

[redacted]

UNCLASSIFIED

Dr. 7769

FIG. 9 PAGE 38

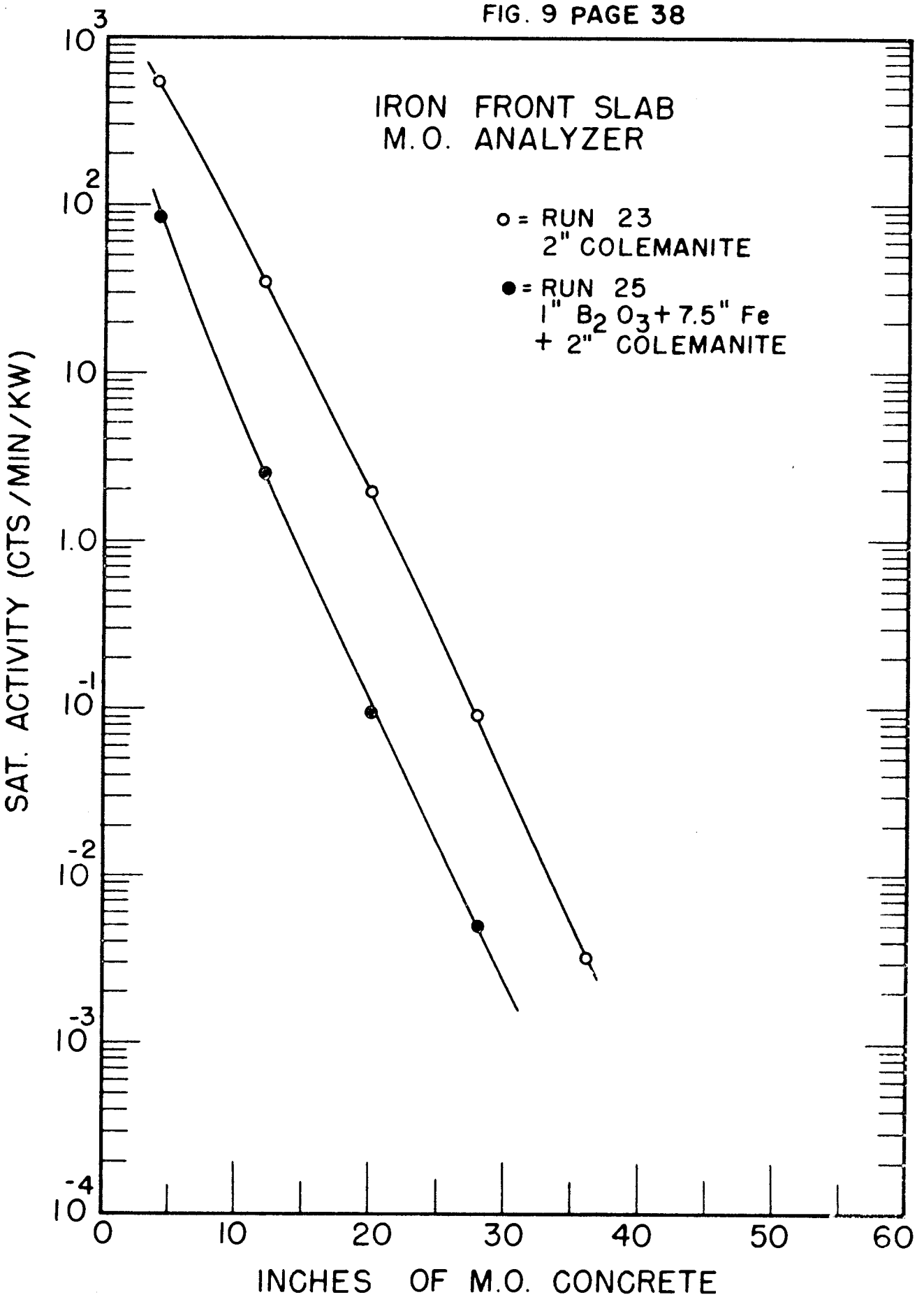

FIG. 10 PAGE 39

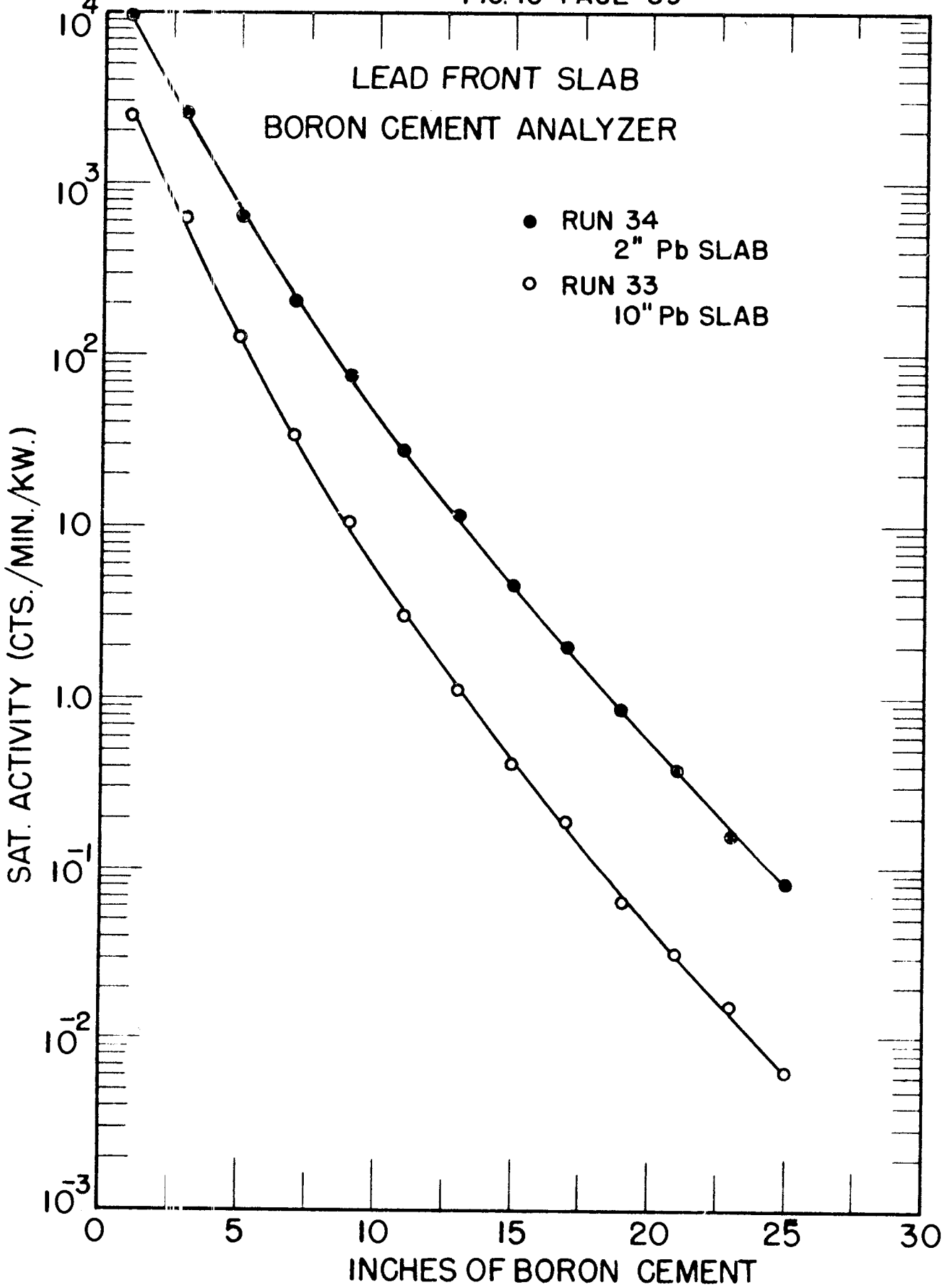

FIG. 11 PAGE 40

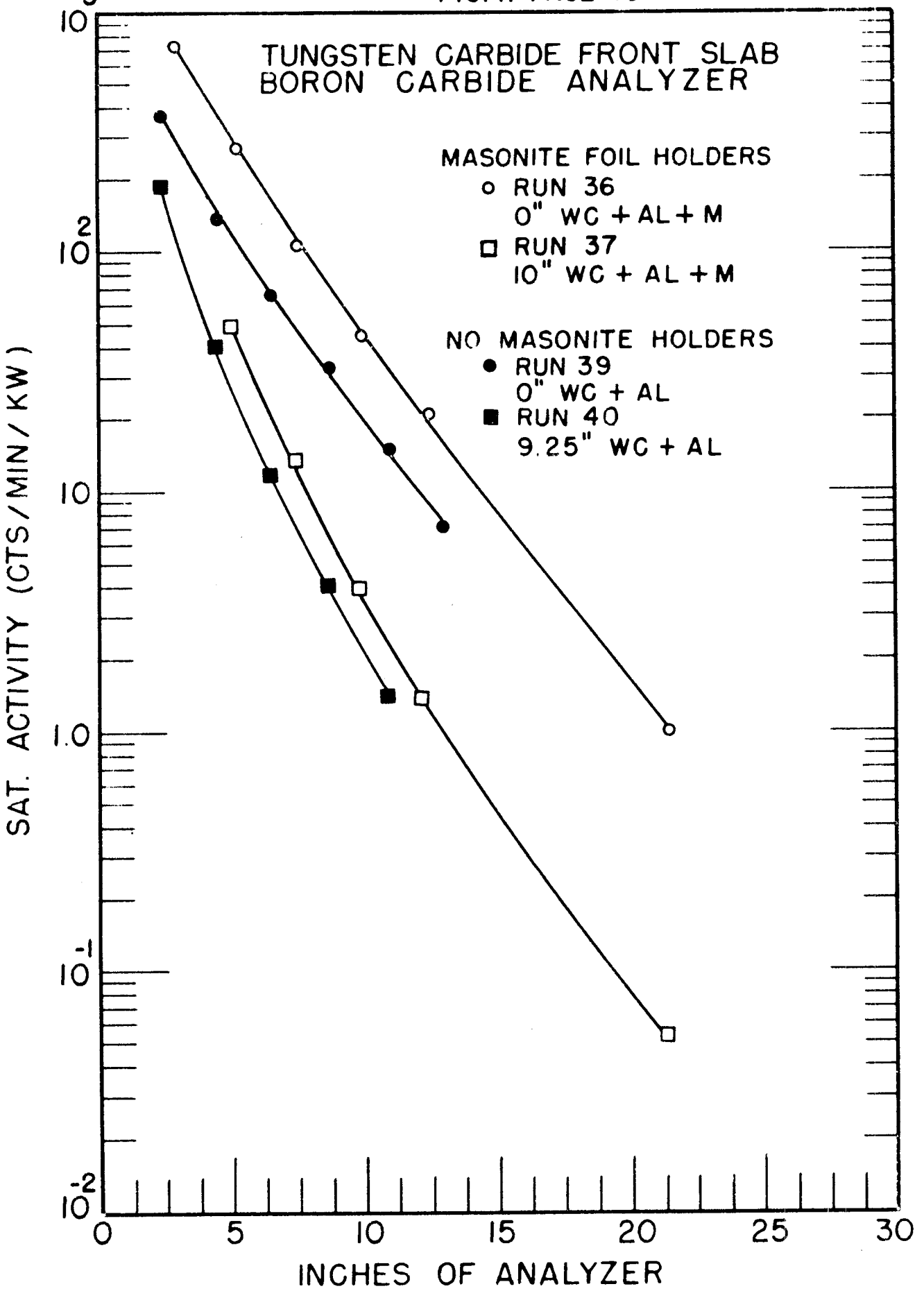

FIG. 12 PAGE 41

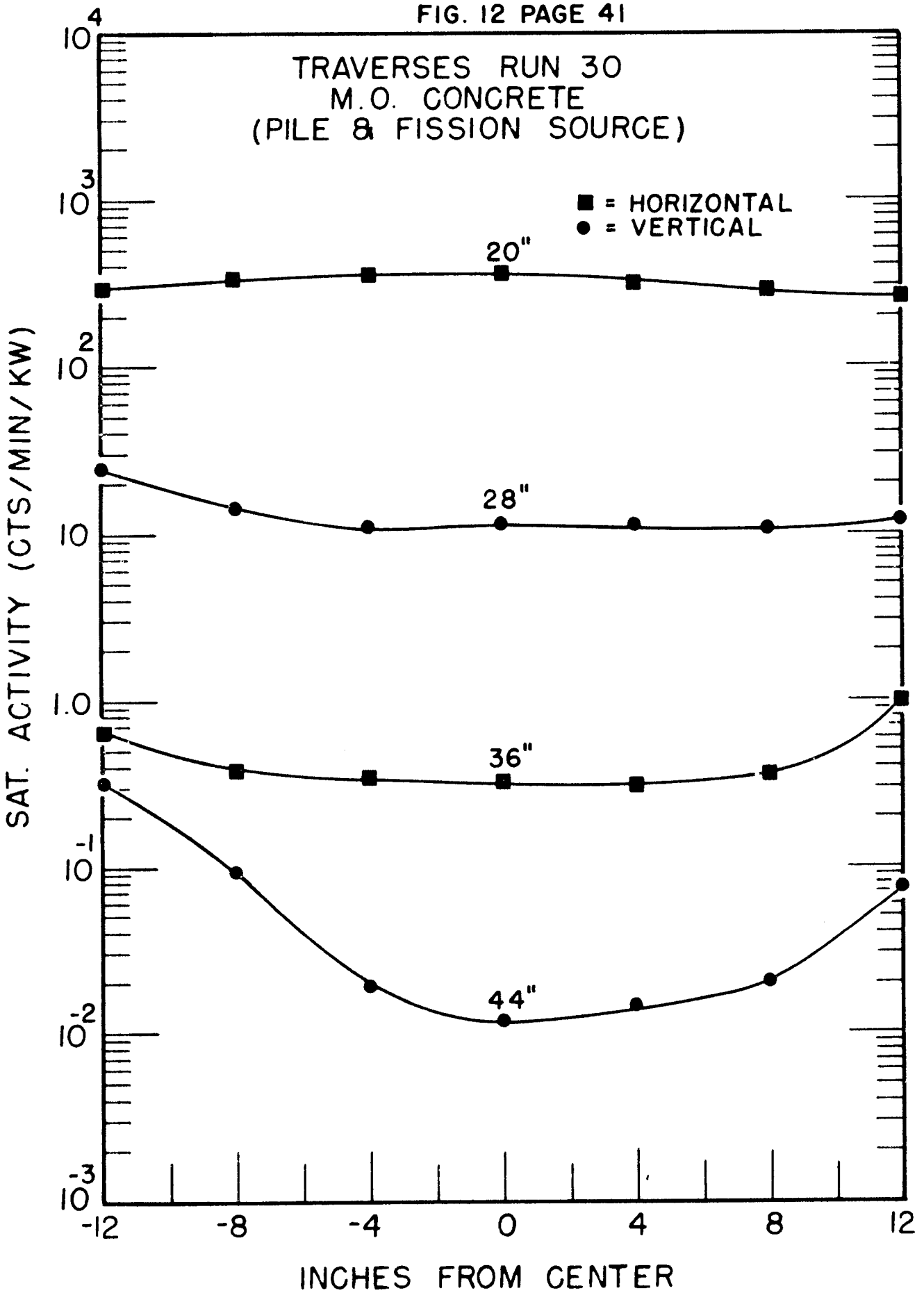

FIG. 13 PAGE 42

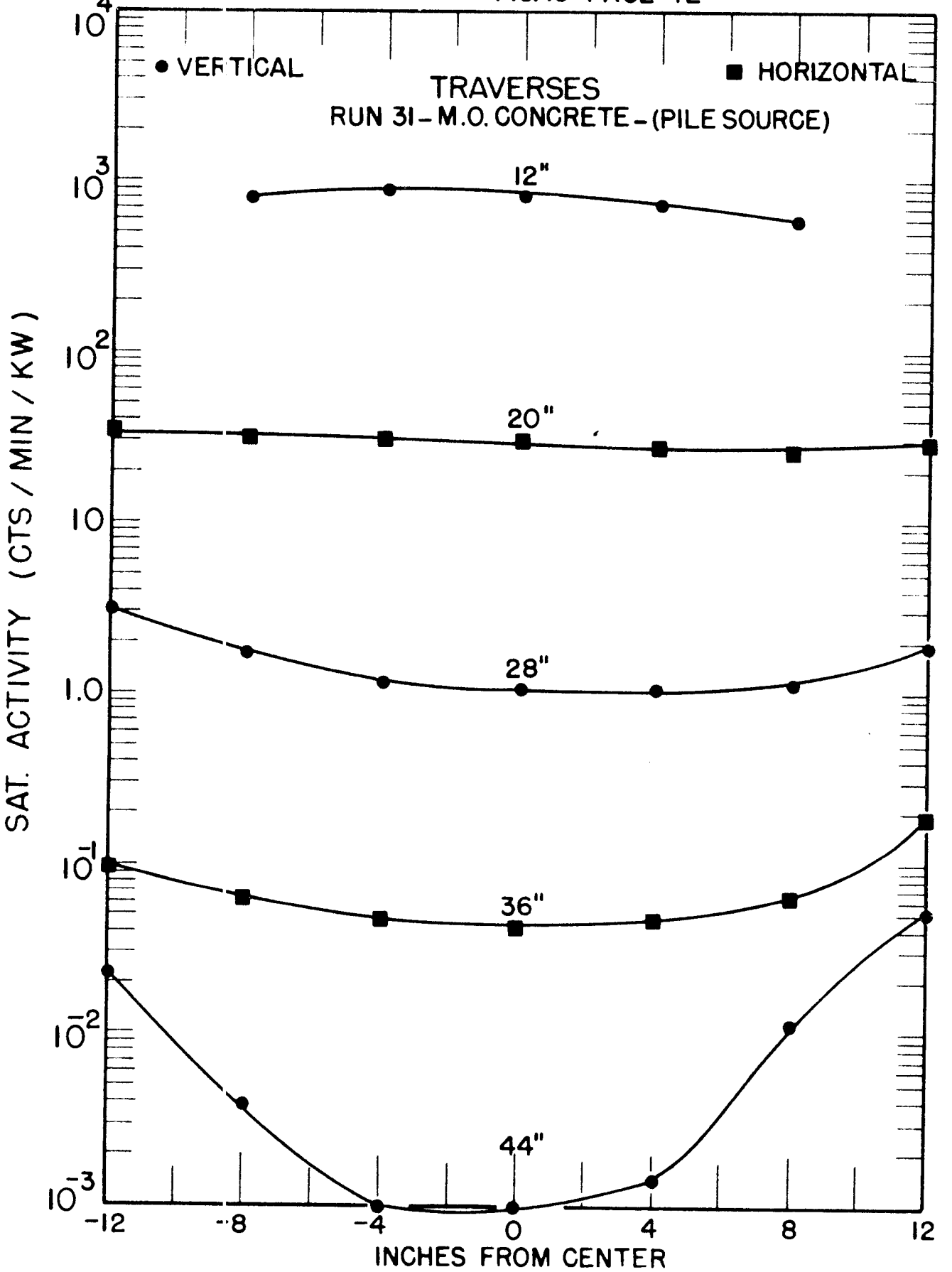

FIG. 14 PAGE 43

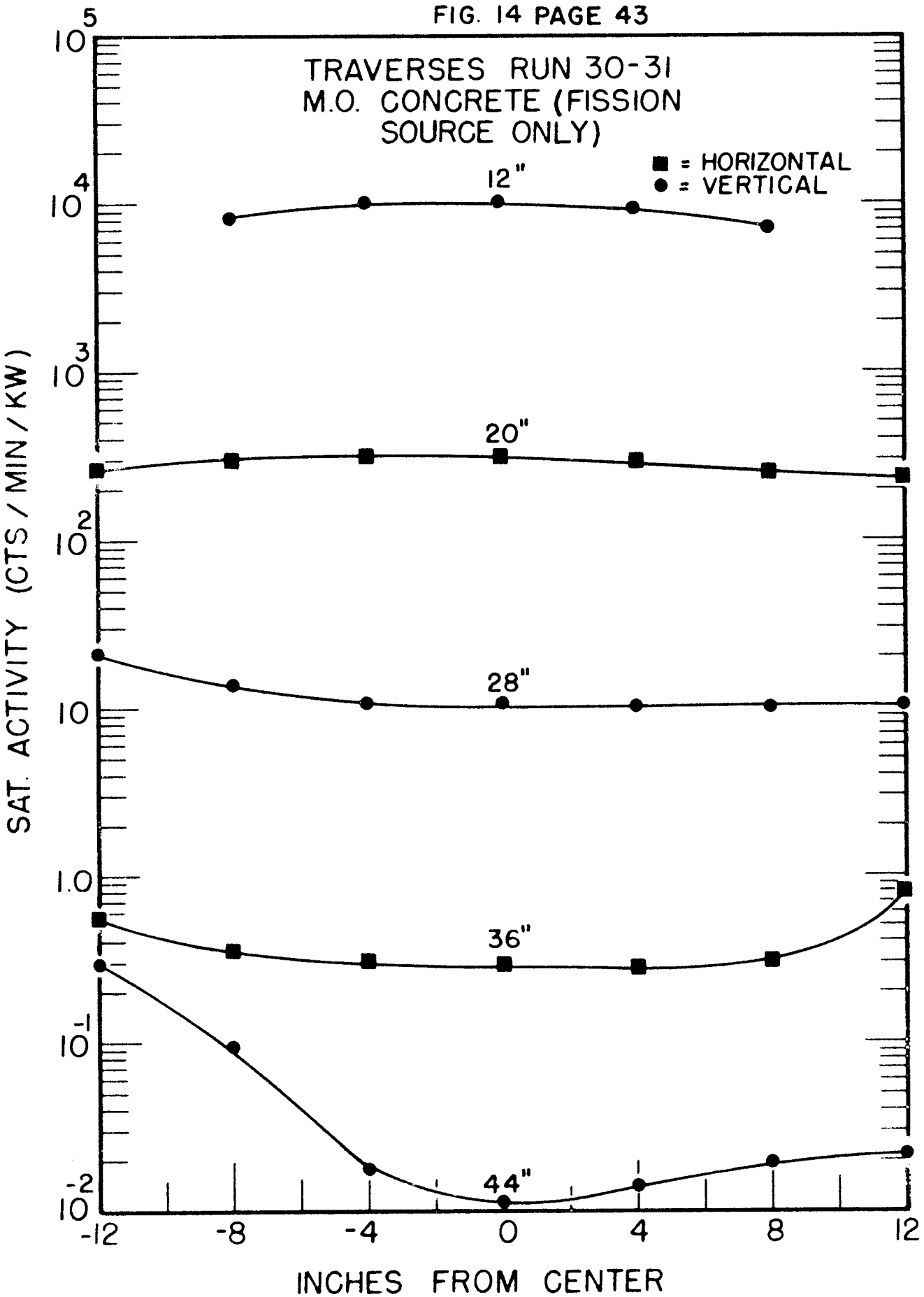

FIG. 15 PAGE 44

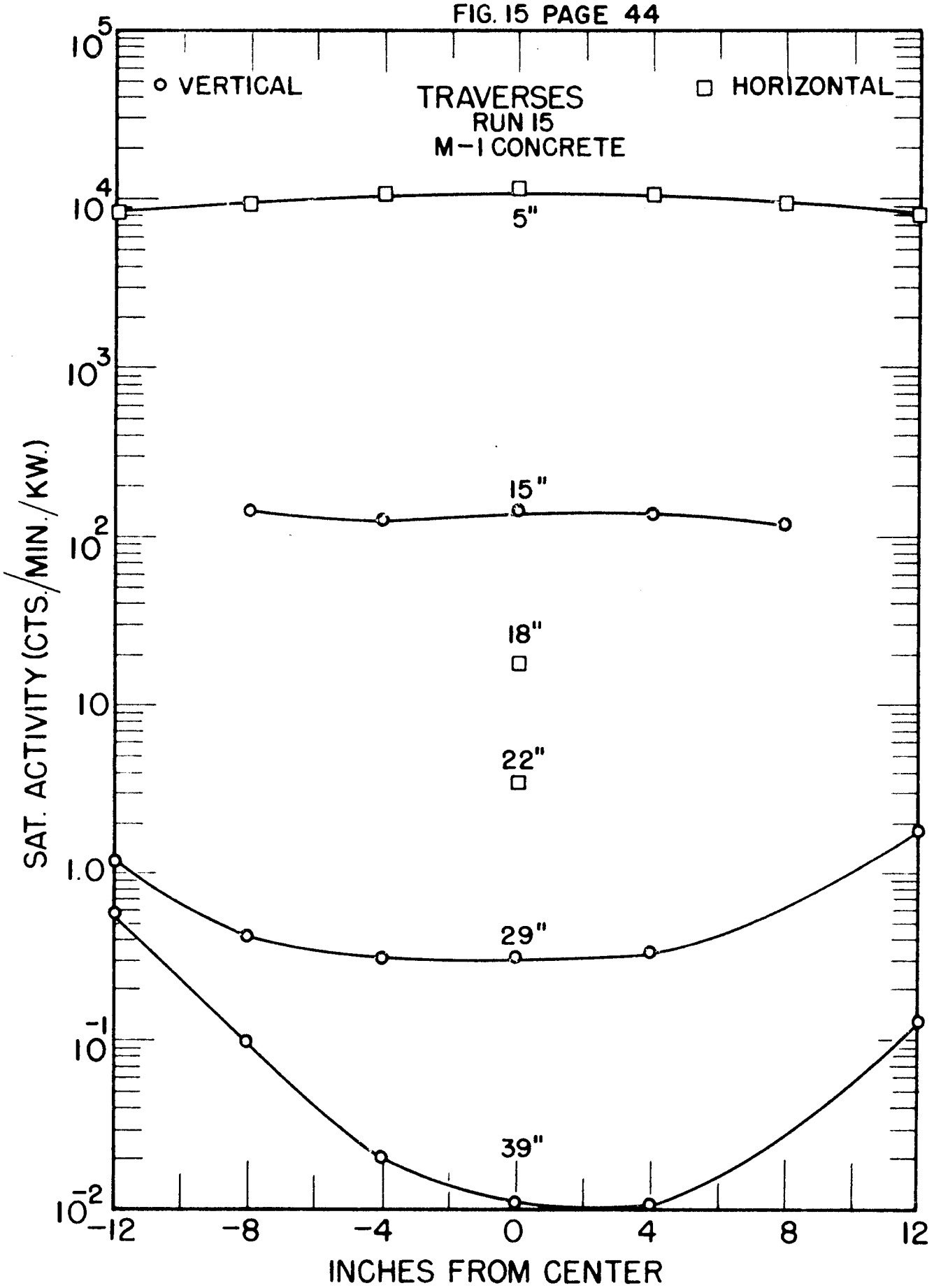

FIG. 16 PAGE 45

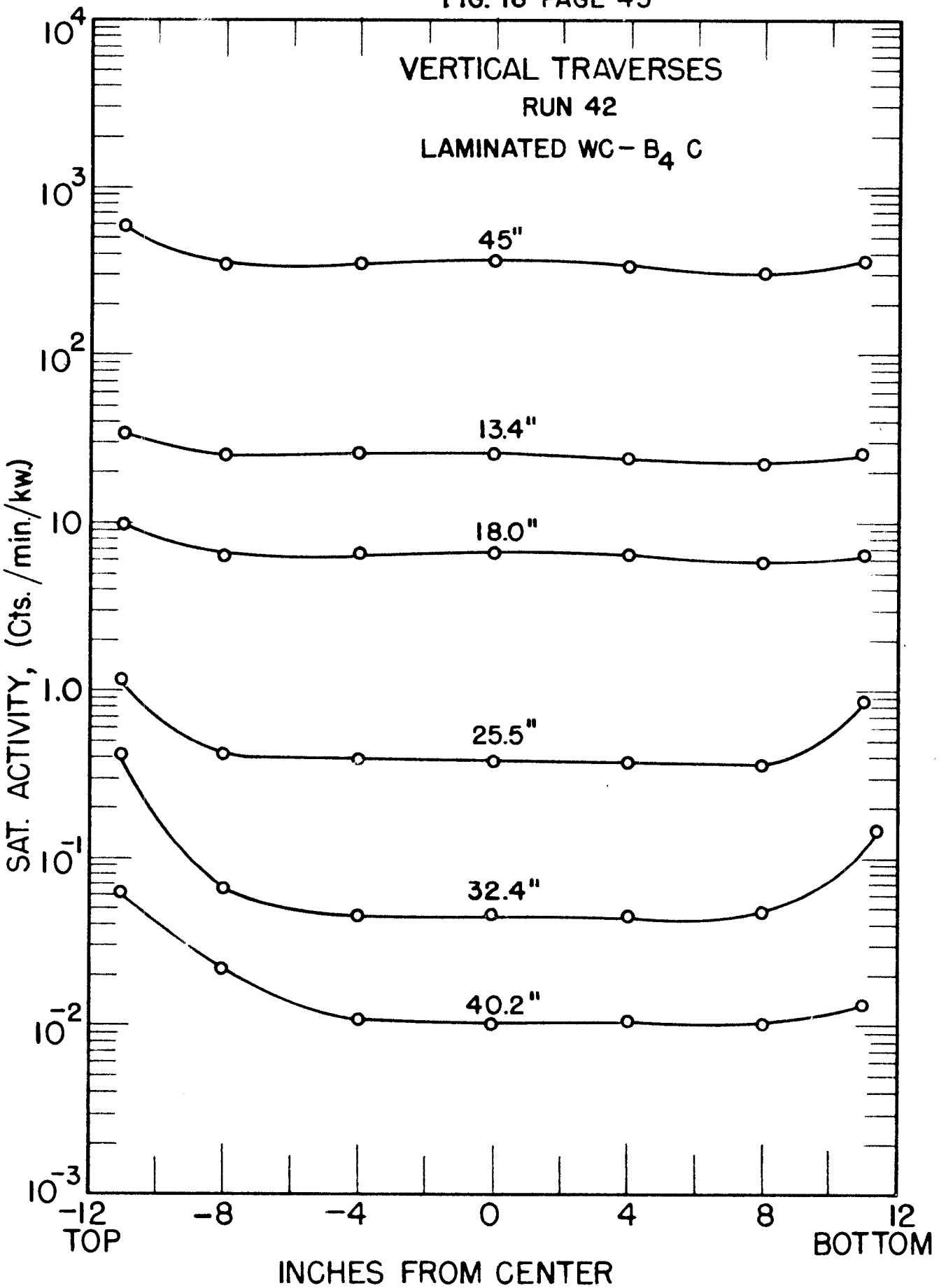

FIG. 17 PAGE 46

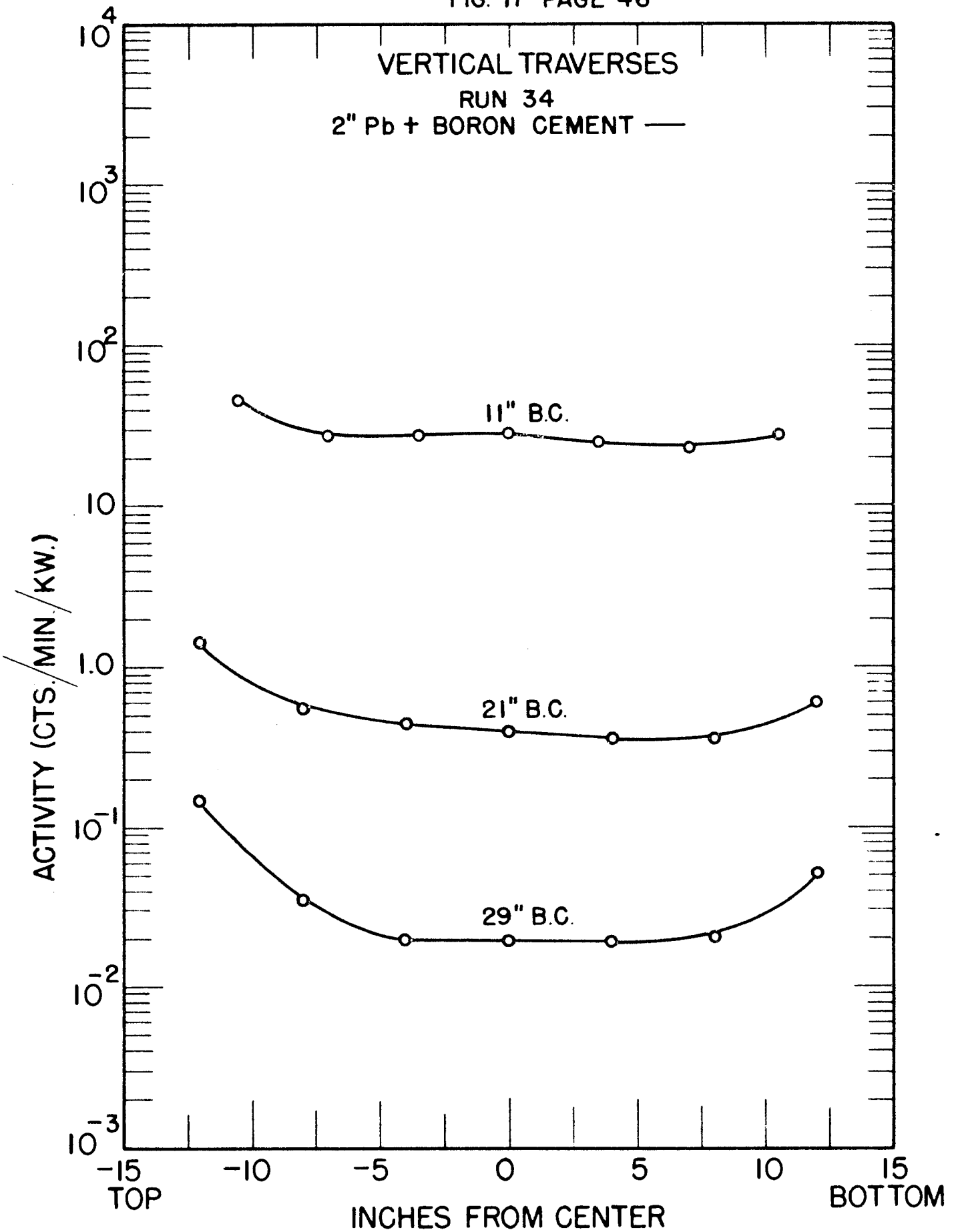

FIG. 18 PAGE 47

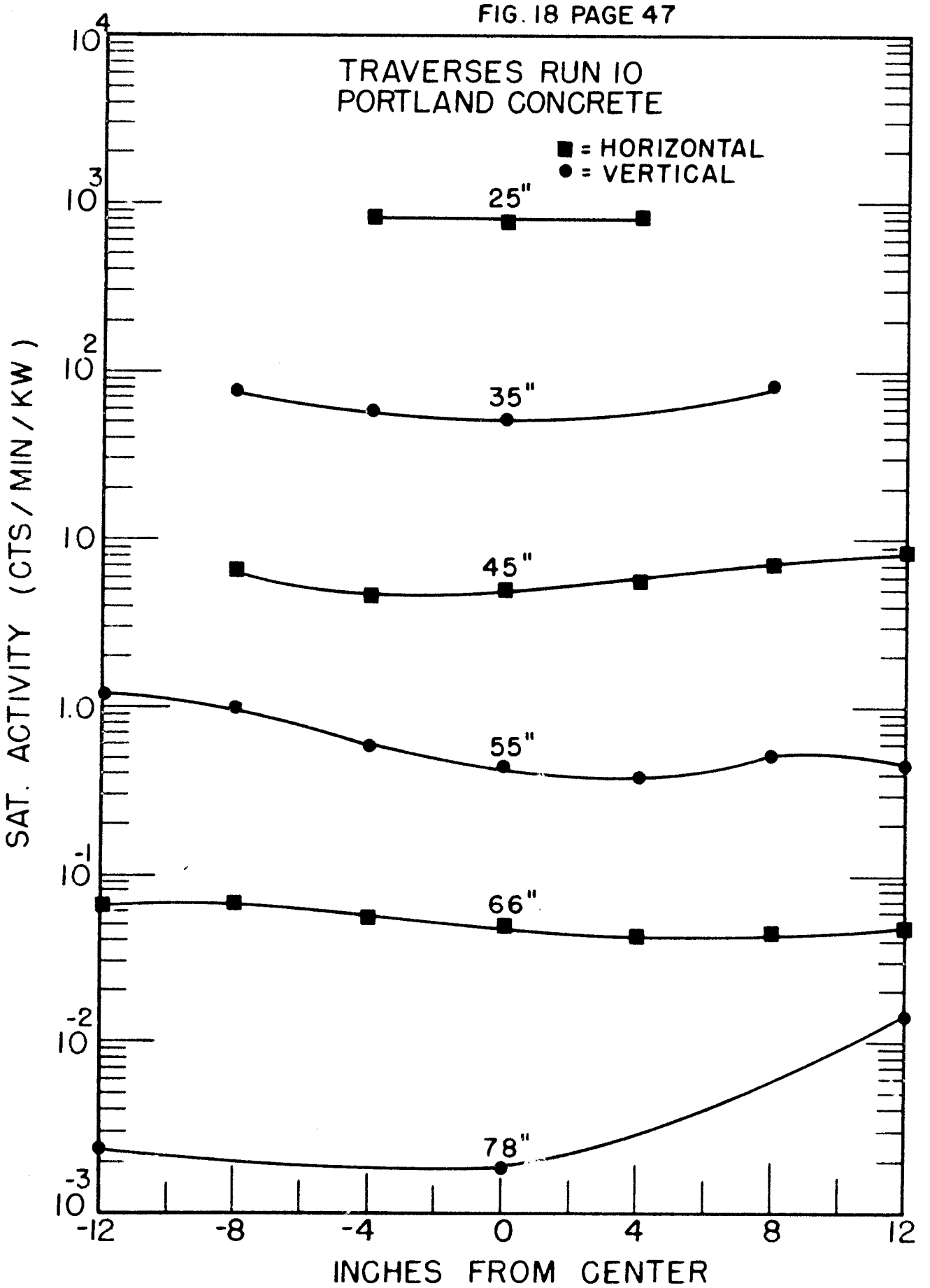
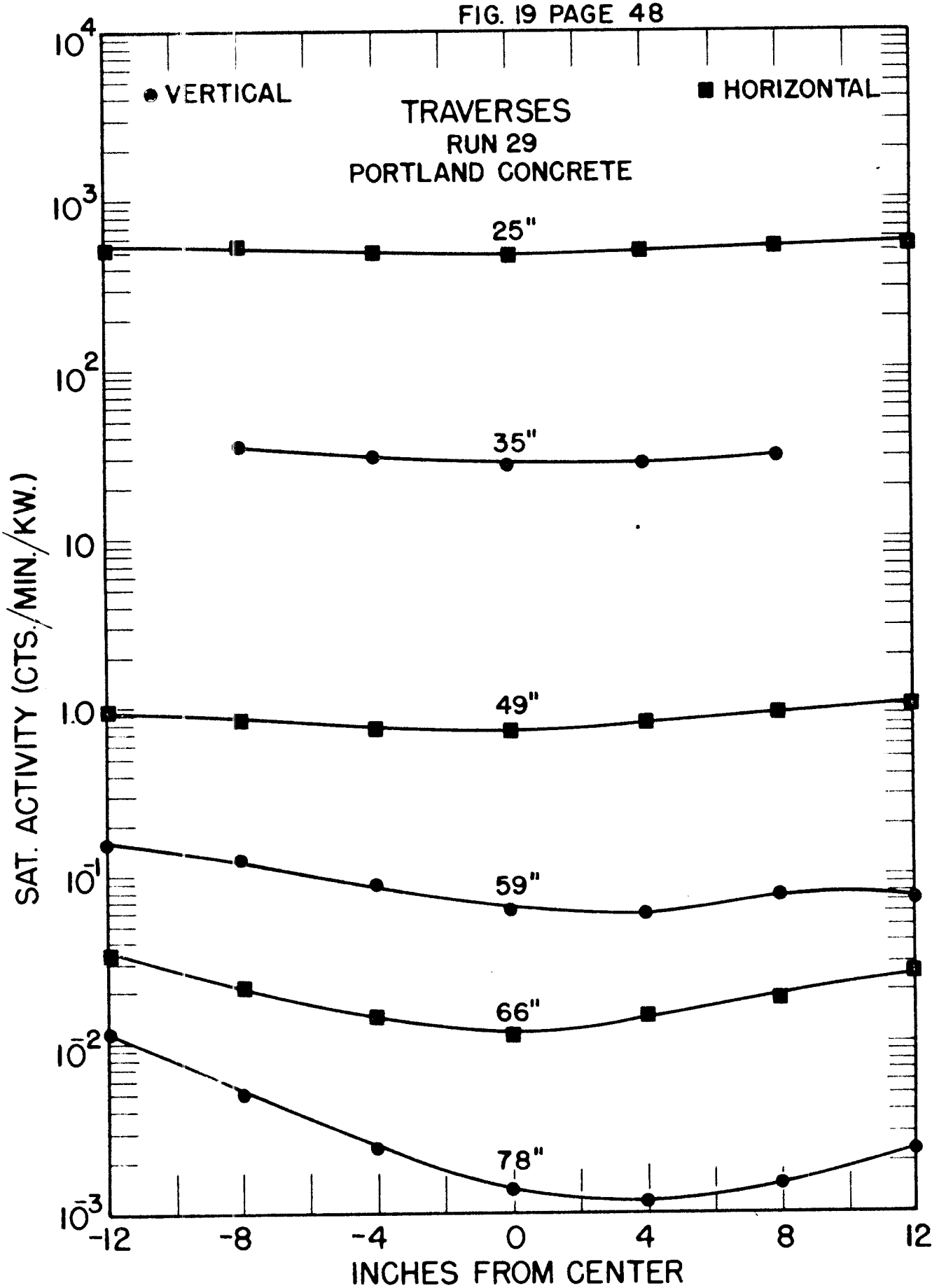
FIG. 19 PAGE 48